NASA CR-421

TECH LIBRARY KAFB, NM

0099580

**NASA CONTRACTOR REPORT**

NASA CR-421
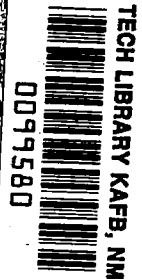
# A REVIEW OF THE PLANFORM EFFECTS ON THE LOW-SPEED AERODYNAMIC CHARACTERISTICS OF TRIANGULAR AND MODIFIED TRIANGULAR WINGS

*by Kenneth Razak and Melvin H. Snyder, Jr.*

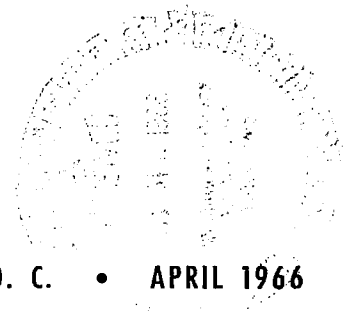NATIONAL AERONAUTICS AND SPACE ADMINISTRATION • WASHINGTON, D. C. • APRIL 1966

A REVIEW OF THE PLANFORM EFFECTS ON THE LOW-SPEED

AERODYNAMIC CHARACTERISTICS OF TRIANGULAR

AND MODIFIED TRIANGULAR WINGS

By Kenneth Razak and Melvin H. Snyder, Jr.

# C O N T E N T S

iii
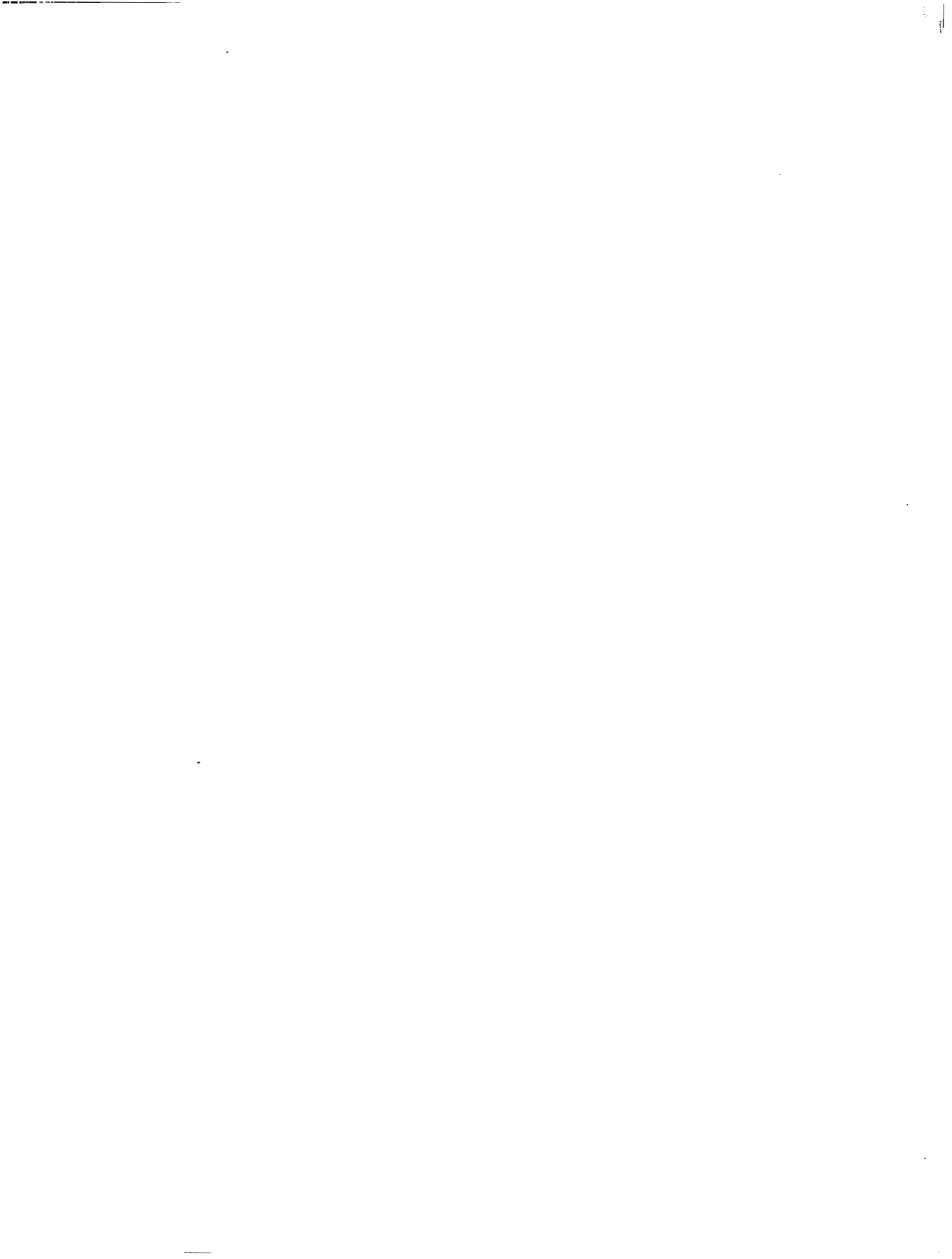
SYMBOLS

| | | |
|---|---|---|
| A | aspect ratio, $A = \dfrac{b^2}{S}$ | |
| a | half-wing span at the chordwise station $x \cos \alpha$ | (ft.) |
| $a_i$ | semispan of the $i^{th}$ rectangular wing element | (ft.) |
| $a_0$ | section lift curve slope, $\dfrac{dC_\ell}{d\alpha}$ | |
| a.c. | aerodynamic center | (% of $\bar{c}$) |
| b | span of wing | (ft.) |
| $C_D$ | coefficient of drag, $\dfrac{D}{qS}$ | |
| $C_{D_i}$ | induced drag coefficient, $\dfrac{D_i}{qS}$ | |
| $C_{D_0}$ | parasite drag coefficient, $C_D$ at $C_L = 0$ | |
| $C_L$ | coefficient of lift, $\dfrac{L}{qS}$ | |
| $C_{L_\alpha}$ | slope of lift curve, $C_{L_\alpha} = \dfrac{dC_L}{d\alpha}$ at $C_L = 0$ | |
| $C_\ell$ | section lift coefficient | |
| $C_m$ | airplane pitching moment coefficient, $C_m = \dfrac{M_{a.c.}}{qS\bar{c}}$ | |
| $C_N$ | $\dfrac{N}{qS}$ | |
| c | local chord | (ft.) |
| $\bar{c}$ | mean aerodynamic chord | (ft.) |
| $c_r$ | root chord | (ft.) |
| $c_t$ | tip chord | (ft.) |
| $c_\ell$ | section lift coefficient | |
| c.p. | center of pressure | (% of $\bar{c}$) |
| D | drag | (lb.) |
| $D_i$ | induced drag, $D - D_0$ | (lb.) |
| $D_0$ | drag at zero lift | (lb.) |
| L | lift | (lb.) |
| $\ell$ | linear dimension | (ft.) |

| M | Mach number, $M = \dfrac{V}{49.04\sqrt{T}}$ | |
|---|---|---|
| $M_{a.c.}$ | pitching moment about a.c. | (ft.-lb.) |
| N | component of aerodynamic force normal to wing m.a.c. | (lb.) |
| n | fraction of distance between successive bound vortices | |
| $n_w$ | number of rectangular wing elements | |
| P | wing semiperimeter | (ft.) |
| p | pressure | (lb./sq. ft.) |
| $p_c$ | pressure coefficient, $p_c = \dfrac{p_{local} - p_{free\ stream}}{q}$ | |
| q | dynamic pressure, $q = \dfrac{1}{2}\rho V^2$ | (lb./sq. ft.) |
| R | Reynolds number, $R = \dfrac{\rho V \ell}{\mu}$ | |
| r | airfoil section leading-edge radius | (ft.) |
| S | wing planform area | (sq. ft.) |
| T | absolute temperature (free air) | (deg. R) |
| t | airfoil maximum thickness | (ft.) |
| $t_x$ | airfoil thickness at chord station x | (ft.) |
| V | velocity (free-stream) | (ft./sec.) |
| v | local velocity | (ft./sec.) |
| x | distance measured in direction of free-stream velocity | (ft.) |
| y | distance measured normal to free-stream flow and parallel to wing span | (ft.) |
| z | distance measured normal to x and y | (ft.) |
| $\alpha$ | angle of attack | (deg.) |
| $\alpha_{L=0}$ | angle of attack for which wing lift is zero | (deg.) |
| $\Gamma$ | circulation, $\oint v \cdot d\ell$ | (sq. ft./sec.) |
| $\gamma_n$ | Fourier coefficient | |

| | | |
|---|---|---|
| $\Delta$ | increment | |
| $\delta$ | surface deflection angle | (deg.) |
| $\varepsilon$ | wing planform semi-vertex angle | (deg.) |
| $\theta$ | vortex shedding angle | (deg.) |
| $\Lambda_{c/4}$ | angle of sweepback measured to the line through the section quarter-chords | (deg.) |
| $\Lambda$ | sweepback angle of the leading edge | (deg.) |
| $\lambda$ | taper ratio, $= c_t/c_r$ | |
| $\rho$ | air density | (slugs/cu.ft.) |
| $\psi$ | stream function | |

ABSTRACT

The fundamental aerodynamic phenomona of the flow
around sharp leading edge triangular planform wings is
reviewed.  Analytical methods of predicting lift character-
istics of triangular wings are summarized and experimental
results of tests on wings of various planform are presented.
A bibliography of 258 references is included.

# INTRODUCTION

Aircraft designed for transonic and supersonic flight require the use of delta, double-delta, arrow, or other highly swept wings having triangular, or approximately triangular, planforms. The advent of the supersonic transport makes it mandatory that the aerodynamic characteristics of these wings at low speeds be such that the airplane can use commercial airports. This usage requires accommodation in traffic control systems mixed with present generation jet aircraft traffic; therefore, the airplane must be tractable in the take-off, approach, and landing configurations. The prediction of flight characteristics in these operating configurations requires not only knowledge of $C_{L_{max}}$, L/D and $C_M$ variations at lift coefficients corresponding to approach and take-off speeds, but it is also necessary to be able to estimate side force and yaw derivatives, flow stability, ground effects, and the manner in which these parameters are time-dependent in accelerated maneuvers.

The airflow at low subsonic speeds (M < .3) about a triangular planform wing having a thin cross-section and sharp leading-edge is a complex mixture of many flows which are individually definable but which, when interacting, are almost impossible to analyze. This complexity causes the triangular wing to differ distinctly from wings having larger aspect ratio, such as the rectangular or tapered

2

unswept wing and the conventional swept wing. Whereas unique procedures are available for the design and aerodynamic analysis of each of these foregoing wing types, the extreme complexity of the flow around a triangular wing at moderate or high angles of attack (usually > 15°) has made it difficult to evolve either a single or a combination of theories which can be dependably used for design.

NASA has, from time to time, surveyed and summarized the state of the art in certain aerodynamic areas. Notable reports are a summary of airfoil data (Ref. 1), a survey of swept wings (Ref. 100) and a review of the stall characteristics of swept wings (Ref. 2). The following report is a review of the state of the art with respect to the theoretical and experimental investigation of the aerodynamic characteristics of triangular or modified triangular wings. It has been determined, unfortunately, that it is not possible to present a complete summary, but an attempt has been made to give a description of the physical phenomena of the flow on the basis that a more complete understanding of the qualitative flow field will assist in interpreting the summary data which has been collected.

No attempt has been made to evaluate any of the wing planforms as to their desirability for supersonic operation. It is presumed that the requirements for supersonic operation are

overwhelmingly predominant and the choice of configuration will be made to satisfy these criteria. It is probable that the configuration will be such that the flow will include such phenomena as leading-edge vortex shedding, streamwise boundary-layer separation lines, and a complex combination of trailing-edge vortex and conical vortex interaction. It might be said that this report pertains to those wings on which streamwise shedding of vorticity from the swept leading-edge is the common characteristic and on which this shed vorticity radically affects the total flow pattern.

This report consists basically of two parts--first, a discussion and analysis of the flow field about triangular wings and the effects of that flow on the low-speed aerodynamic characteristics of the wings, and, second, an analysis of published empirical data to determine wing planform effects on the aerodynamic characteristics.

Classified material has not been surveyed in this summary study, and, therefore, very little of the latest test data on triangular or variable sweep wings has been included. Since extensive experimental work has occurred on different versions of the SST, it is presumed that a body of literature exists which will, at some later time, permit a correlation of some of the analytical and general theories with experimental results. This correlation is now not possible in an unclassified document.

# THE FLOW FIELD ABOUT A TRIANGULAR WING

Extensive literature is available, as seen in the bibliography (Refs. 8-58) in which methods are given to predict $dC_L/d\alpha$, $C_{L_{max}}$, $C_{D_0}$, $C_{D_i}$, $C_m$, and L/D characteristics of straight wings, swept wings, and even slender bodies serving as lifting surfaces. The work of De Young and Harper (Refs. 18, 19, and 20) extending and amplifying Weissinger's method of predicting span loadings and the work of Lowry and Polhamus (Ref. 179) which further refines the method of estimating lift increments due to flap deflections are examples of this well-developed literature. The work of Sacks, Nielson, and Goodwin (Ref. 48) and Brown and Michael (Refs. 11 and 12) give admittedly incomplete and approximate methods of predicting the characteristics of triangular planform wings.

The aerodynamic feature of the delta or modified delta wings which distinguishes them from other wings is the leading-edge shedding of vorticity. This feature is illustrated in the sequence of sketches in figure 2 which diagramatically illustrate the manner in which vorticity is shed from a variety of wings. Figure 2(a) shows a rectangular plan wing with a series of bound vortices and spanwise continuous shedding of vortex filaments aligned with the local flow at the trailing-edge. A vortex filament is defined as a line along which the

5

entire vorticity of a vortex can be assummed to be con-
centrated, with the vector sense of vorticity determined
by the right-hand rule. The strength of a vortex $\Gamma = \oint \bar{v} \cdot d\bar{\ell}$,
is identified as a vector directed along the filament.

The span loading of the wing is a measure of the
strength of the bound vorticity at all span stations. With
a non-uniform span loading, the increment of loading, $\Delta(C_\ell c)$,
between any two span stations is directly proportional to
the magnitude of vorticity shed between those two stations.
The vortex filaments must align with the local flow at the
point of shedding, and eventually trail off downstream in
the free stream direction. The intensity, or density, of
the vortex filament sheet is proportional to the slope of a
tangent to the span loading curve at each point along the
span $(d\Gamma/dy)$.

The bound vortices which extend along the complete span,
from wing tip to wing tip, are shed at the tip, and, therefore,
a concentrated vortex region exists at that point. The
details of this shedding and the subsequent roll-up of the
vortex sheet are graphically illustrated and analytically
described in reference 83.

Vorticity need not always be shed with the vortex filament
aligned with the local flow, however. When the boundary layer
growth has become such that the decreased kinetic energy in
the boundary layer is insufficient to move it against an

adverse pressure gradient, the boundary-layer velocity profile is altered so that $\frac{dv}{dy} = 0$ at the wing surface. At this separation point, the streamline is normal to the surface, thus, the airflow at that point is also normal to, and away from, the surface. The vorticity which has been generated in the boundary layer upstream of the separation point, with a spanwise vortex filament, also flows away from the surface since it must remain associated with the fluid in which it has developed. The vector sense of this shed vorticity is the same as that of the bound vorticity. The total strength of the bound vorticity is therefore reduced as the boundary layer vorticity is shed and the lift over this portion of the wing is reduced. Figure 2(b) illustrates the closed vortex systems which would be shed by a wing with intermittent stall near the trailing edge.

Küchemann, in reference 71, discusses, at length, the various types of vortex flow which occur on swept and triangular wings and pays attention to the interaction of sheet vorticity and boundary layer growth. With reference to swept wings, i.e., wings of finite taper ratio as contrasted with triangular wings which have taper ratio of zero (or nearly zero), the remarks of Küchemann are valuable in developing an understanding of the aerodynamic phenomena which produce the characteristics of swept wings as summarized by Harper and Maki in reference 2.

Küchemann pays particular attention, however, to the
vortex sheets which are shed either at the wing tip or at
partial-span stations and differentiates between vortex
sheets which are shed as a result of boundary layer phenomena
and those which are shed as a result of invoking the Kutta
condition at the leading edge.  It is usually necessary
to invoke the Kutta condition at the leading-edge of a
delta wing because a delta wing, having a small aspect ratio,
necessarily has a small relative airfoil thickness and a
sharp leading-edge.

A vortex sheet is defined as an infinite number of vortex
filaments, placed side by side, each of which has an
infinitesimal strength.  The strength of the vortex sheet is
the circulation integrated across the width of the sheet.

The condition of small relative thickness and sharp
leading-edge requiring the Kutta condition at the leading-
edge prevails, also for other small aspect-ratio wings;
arrow, gothic, ogive, and even rectangular.  It will be
shown, later in this report, that modification of the
leading-edge of a delta wing by increasing the effective
leading-edge radius using droop-snoot flaps, significantly
changes the pattern of vortex shedding and the drag due
to lift.

In the case of moderate- and large-span wings, straight or swept, the relative section thickness is usually greater than that of a delta wing, and the leading-edge can be considered rounded, rather than sharp. It would appear, at first consideration, that the difference between a delta wing and a swept-wing is one of planform only; i.e., a swept-wing is a delta-wing with a swept trailing-edge. The important difference is, however, the condition of the leading-edge.

For the purpose of this report, delta wings (chiefly with sharp-leading edges) and modifications of delta wings such as arrow wings and sharp-edged low-aspect-ratio swept-wings will be called triangular wings. Moderate and high aspect ratio wings (straight or swept, $AR > 4.5$) will be referred to as conventional wings.

From a different point-of-view, triangular wings are those which are most improved aerodynamically by leading-edge modifications (and very little improved by trailing-edge modifications).

The vorticity patterns during the normal lift and stall of three different types of airfoils are shown in figure 3. Figure 3a shows an airfoil, usually at 12% thickness ratio or higher, on which initial boundary layer separation occurs near the trailing-edge and moves forward. In figure 3b, boundary-layer separation occurs very near to the leading-edge, usually where the boundary layer is still laminar,

9

but the boundary layer undergoes transition and the flow re-attaches to the airfoil surface as a turbulent boundary layer. Figure 3c shows the case where boundary-layer separation occurs at or near the leading-edge but the flow does not re-attach and a turbulent bubble extends beyond the trailing-edge.

The important point to note is that in cases A and C the separated vortex sheet carries away with it vorticity of the same direction as the bound vortex. This separated vorticity is part of the previously bound vortex and this action reduces the strength of the bound vortex and the net lift of the wing. In other words, only the bound vorticity produces lift ($L/b = \rho V \Gamma_b$) and this bound vorticity is weakened by the separated vortex sheet. It should be noted that the vortex filaments are still parallel to the span in all cases.

In case B, the chordwise extent and vertical displacement of the separated vortex sheet is so small that little effect is felt upon the airfoil lift or pressure distribution. The main consequence is that energy is dissipated in the small detached vortex region, and this energy loss makes the boundary layer susceptible to earlier downstream separation. Thus, the leading-edge bubble acts to reduce section $C_{\ell_{max}}$.

On a finite span wing, boundary layer separation does not necessarily occur along the entire span. In fact, a wing designer will strive to cause stall to occur in a limited region, hopefully inboard, so that the aircraft will have satisfactory pitch and control characteristics. The disposition of vorticity along the span will be that as shown in figure 4. Since the lift over the portion of the span where stall has occurred will be less, the bound vorticity on the unstalled portion must trail off downstream in accordance with the theory of continuity of vorticity. A rear view of the wing will show the conventional sheet of shed vorticity disposed in the plane of the wing but will also show a vertically disposed vortex sheet located at the discontinuity between the stalled and unstalled portion of the wing. The interaction of the horizontal and vertical vortex sheets not only modifies the spanwise distribution of the load on the wing but also changes the downwash characteristics at the horizontal tail. The vortex shedding associated with tip stall may increase the downwash at the tail, and thus aggravate nosing-up characteristics, whereas inboard stall will reduce downwash and produce a nose-down tendency.

The nature of boundary-layer growth and separation can be seen to influence the pattern of shed vorticity. In the case of conventional swept-wings, the spanwise flow in the boundary layer aggravates boundary-layer growth at

the tips while producing a form of stall-delaying boundary-layer control on the inboard sections. This motion leads to boundary-layer separation outboard with a shedding of a part-span vertical vortex sheet. Both the loss of lift on the tip area aft of the center of gravity, and the increased downwash from the smaller span vortex sheets, induce unstable pitching-up moments. Extensive efforts, as summarized in reference 2, have been exerted to relieve, if not remedy, this characteristic.

The nature of vortex shedding is basically different between a conventional wing and a triangular wing as is shown in figure 5. All characteristics, lift, drag, and pitching moment, are substantially different; these differences result from the different vortex sheets shed by each wing. Whereas the Kutta condition is invoked at the trailing-edge and tips of the conventional wing, it is invoked at the leading-edge of the triangular wing. Whereas the conventional wing undergoes a variety of vortex shedding patterns from zero lift to the stall, the vortex pattern of the triangular wing is stabilized at a small angle of attack and remains constant in pattern up to the stall, merely increasing in strength and shifting position slightly. Whereas the vortex patterns of a straight or moderately swept wing become stabilized into a mathematically predictable pattern once "roll-up" has occurred, the vortex

patterns of a thin delta wing undergo a combination of inter-
actions with secondary vortices and are subject to a phenomena
called "bursting" or "exploding." Whereas the lift-curve
slope for a conventional wing is greatest at small lift
coefficients, the lift curve slope for the triangular wing
increases with lift coefficient until stall begins. Whereas
the lift curve may break suddenly at the stall of a con-
ventional wing, the peak of the lift curve is rounded for
a delta and occurs at angles of attack of 30° or higher.

The section of the bibliography on general description
of the flow and flow visualization, references 59 to 87,
illustrates the extensive effort that is being expended to
explore and understand the fundamental phenomena of the
flow around triangular planform wings. An interesting
experiment is described by Werle in reference 87 in which
colored fluid was emitted from the surface of a 60°
delta wing in a hydrodynamic flow facility. The filaments
of colored fluid demonstrated the typical separated
conical vortex flow, but at speeds of 5 to 10 cm/sec (.15
to .3 ft/sec) the fluid filaments were observed to "explode"
into a diffuse turbulent pattern in a manner very similar to
the sudden and classic transition from laminar to turbulent
flow of a laminar flow in a tube at the critical Reynolds
Number. It was found that external influences such as suction
in the region of the trailing edge, a barrier aft of the

trailing edge, or changing angle of attack all affected the point of the "explosion."

References 73 and 87 give an unusually graphic description of the burst phenomenon in which the spiral vortex sheet suddently transforms from a well-defined orderly spiral motion, almost laminar in nature, to a larger diameter turbulent and diffused vortex with a velocity distribution across it much more like that of a single vortex. The phenomenon of vortex breakdown has been explored by other investigators, references 72 to 76 and reference 81. Breakdown occurs at all Reynolds Numbers and Mach Numbers but little or no information was found which related the breakdown phenomenon to the force or moment characteristics at the time of breakdown. Many questions can be posed regarding the specific consequences of vortex breakdown and it appears that an investigation of these questions is needed.

Most of the material reviewed in this section of the report covers work which was done at very small Reynolds Numbers, some as low as $10^5$, others in the range of $1 \times 10^6$ to $4 \times 10^6$. This range is considerably different from operating Reynolds Numbers of over $10^8$. It is in order to note that caution should be observed in interpreting wing flow phenomena at low Reynolds Numbers. This same point is emphasized in observing figures 5 and 6 of reference 63 in

which the flow at the trailing-edge of a delta wing in a hydrodynamic tunnel was radically affected by the boundary layer on the wall of a semi-span model.  Nevertheless, such tests are useful in depicting gross flow patterns and can serve as a guide for more quantitative tests.

METHODS OF ANALYSIS FOR TRIANGULAR WINGS

As mentioned previously, the distinguishing feature of flow about a lifting triangular wing is the leading-edge shedding of vorticity. Various persons have offered analyses of this type of flow.

Wing analysis usually consists of establishing a model of the combination of the bound and trailing vortex system, defining (or assuming) the orientation and strength of the vortex filaments and stating the boundary conditions. The boundary conditions include the statement of no-flow through the solid surface of the wing and the condition of tangential flow at a sharp trailing, side, or leading-edge. References 48, 71, and 83 discuss the great variety of vortex systems which exist about lifting wings and references 48 and 83, in particular, advance theories for calculating downwash and span loadings for triangular wings. No attempt will be made to summarize these references. Instead, an attempt will be made to describe the vortex systems which are shed by a triangular wing at increasing angles of attack and to relate these patterns to the aerodynamic results.

One of the more meaningful models is advanced by Sacks, Nielsen, and Goodwin in reference 48. They postulate that the triangular wing can be approximated by a series of rectangular planform wings of varying aspect ratio, the most forward wing being the smallest. Each rectangular

16

wing sheds vortex filaments at its side edges (or wing tips) in accordance with conventional straight wing theory and these vortex filaments trail downstream, since, in accordance with Helmholtz's theorem, they must remain associated with the actual fluid in which they developed.

Another view which may be taken of the vortex field is that of a series of horseshoe vortex filaments of increasing span and decreasing altitude in the direction of the free-stream flow (Fig. 6). The vortex filament which trails downstream from wing element $x_1$ lies inboard and above the vortex filament which trails downstream from the next wing element $x_2$. Successive segments of trailing vortex filament from $x_1$ are, therefore, in the influence of the upwash of the bound vortex at $x_2$, and, for the time element represented by $\frac{x_1 - x_2}{V}$, the vortex filament segment is deflected upward at a velocity given by

$$v_{z_{x_1}} = \frac{\Gamma_{x_2}}{(x_1 - x_2) \, n}$$

where n is the fraction of the distance from $x_1$ to $x_2$ at which the vortex filament segment is located. The velocity increases as the vortex filament segment from $x_1$ approaches the bound vortex at $x_2$ and the trajectory of the vortex filament $\Gamma_{x_1}$ is curved upward from the point of shedding.

When a segment of the vortex filament $\Gamma x_1$ is at or aft of the position of the shedding of vortex filament $\Gamma x_2$, the $x_1$ segment comes into the downwash field of both the bound and the trailing portion of filament at $x_2$ and the trajectory of filament $\Gamma x_1$, is then downward and outward with the effect of the bound vortex at $x_2$ decreasing and finally being counteracted by the next bound vortex at $x_3$. It may be deduced, as the physical model of a discrete number of bound vortices approaches the mathematical model of an infinite number of bound vortices, that the deviation of the trailing vortex filament from the surface of the wing is established at the time of initial separation of the vortex filament from the leading-edge and that the trajectory of the filament, or bundle of filaments, remains constant with respect to the wing surface. Such a conclusion is supported by measurements made by Bergesen and Porter at Princeton University (Ref. 10) which show that the deviation of the vortex core from the wing surface is at an angle of .17 to .25 of the free stream angle of attack for a distance back to 80% of the root chord for delta wings of an aspect ratio of unity.

The trajectory of the vortex filaments, after the influence of the bound vortices has become small, is a function of the lateral spacing and strength of successive downstream shed vortices. A transverse section on figure 6 between stations

18

$x_2$ and $x_3$, as shown in figure 7a, illustrates how the vortex filaments, shed respectively at $x_1$ and $x_2$, interact with each other, each spiralling about the other. Figure 7b is a transverse section at a point farther downstream between stations $x_4$ and $x_5$ which illustrates how the two succeeding vortex filaments shed at $x_3$ and $x_4$ also become involved in the spiralling motion.

The concept of a unique number of bound vortices, each with its continuing trailing vortex filament, is a useful mathematical approximation but the vorticity is actually shed in a continuous sheet at the leading edge so that instead of the separate vortex filaments interacting as in figure 7b, a vortex sheet, as shown in figure 7c, is spirally rolling-up. The "center of gravity" of this spirally wrapped vortex sheet is taken as the "core" of the total vorticity summed along the entire vortex sheet and it is the position of this core which is most often referred to in the literature (see reference 10 in particular).

Werle and Roy of O.N.E.R.A., in their hydrodynamic flow facility, injected vari-colored fluids from the wing surface into the flow about a triangular wing. The "barber pole" appearance of these flow filaments are vivid demonstrations of the shedding of leading-edge vorticity and subsequent roll-up.

# *Error*

---

An error occurred while processing this page. See the system log for more details.

$$\Gamma_i^* = \frac{(d\Gamma/dc)_i\ c}{4\pi a_i\ V_\infty \sin \alpha}$$

$$\gamma_i^* = \frac{{}^n\gamma_n}{4\pi\ a_i V \sin \alpha}$$

$$\psi = \cos^{-1}(-y/a_i)$$

For the case of $C_N$ and $\dfrac{\overline{x}}{c_o}$ , the summation is carried out over the range $i=n$. In the case of the spanwise loading, the summation is carried out over those elements whose span, $a_i$, is greater than the value of $y$ at the chordwise station where the loading is being computed. Specific, step-by-step procedures are given for the computation of the coefficients, $\gamma_n$, and the methods of performing the necessary iterations are given in reference 48. The shedding angle, $\theta/\alpha$ , is a primary parameter which must be secured by iteration or selected from some other appropriate source. Interestingly enough a value of $\theta/\alpha = .75$ is specified as required for an aspect ratio of 1.0 to secure accurate prediction of normal forces, a value which is in remarkable agreement with the test results of Bergesen and Porter (Ref. 10). The vortex shedding angle, $\theta$, becomes smaller with increasing aspect ratios, as shown in figure 18 of reference 48, indicating that the rolled-up vortex core lies closer and closer to the surface as the aspect ratio is increased.

A different basis for arriving at a vortex model was
adopted by Brown and Michael in reference 11.  They recog-
nized the continuous shedding of vorticity at the leading-
edge, but rather than attempt to mathematically treat the
curved surfaces as in figure 8, they established a single
rolled-up vortex core disposed above and inward from the
leading edge with a continuous plane sheet of vorticity feed-
ing the varied along the chord.  The strength of the core
was assumed to be a linear function of x, i.e., $d\Gamma/dx$ = con-
stant and an expression for $C_L$ was developed as follows:

$$\frac{C_1}{\epsilon^2} = \frac{2\pi\alpha}{\epsilon} + 16\pi\left(\frac{\alpha}{4\epsilon}\right)^{5/3}\left[1 + \frac{2}{3}\left(\frac{\alpha}{4\epsilon}\right)^{2/3}\right]$$

This relationship holds for both supersonic and sub-
sonic Mach numbers as long as the leading edge is subsonic
and the result is not affected by viscosity except that
viscosity requires the setting of the Kutta condition at
the leading edge.  Other than this influence of viscosity,
the calculations of both references 10 and 48 are based on
potential flow theory.  The effects of viscosity, however,
are real, and caution should be exercised both in inter-
preting low Reynolds Number smoke or hydrodynamic traces
as well as analytic procedures which ignore the secondary
effects of viscosities.

Bergesen and Porter (Ref 10), through visualization and analytical development, give a good insight into the specific nature of the flow about a delta wing. Figure 9 is taken from their work and illustrates the secondary vortex and the accompanying boundary layer separation which lie below and outboard of the primary spiral vortex sheet. The rotational components about the vortex filaments shed from the leading edge cause an outward flow beneath the conical vortex and a reversal of pressure gradient in the lateral direction occurs immediately below the vortex center. The outward flow, which is induced by the vortex rotation, encounters the adverse pressure gradient below the vortex. The combination of the spanwise growth of the boundary layer and the adverse pressure gradient causes, first, thickening of the boundary layer and, finally, a boundary layer separation along a chord-wise line at angles of attack of about 20°. Since the flow is spanwise, the axes of the vortex filaments in the separated flow are chordwise, and , accordingly, another chordwise vortex gradually grows below, parallel, and outboard of the primary spirally-wrapped vortex sheet.

Figure 10 is a cross-section through the wing at some point intermediate between the apex and the trailing edge. This figure illustrates the double vortex, one resulting from the filaments shed at the leading edge and the other

resulting from spanwise flow separation. Figure 11 illustrates how these two opposing vortices gradually merge aft of the trailing edge.

Bergesen and Porter have examined the lift characteristics of a delta wing and have evolved the following relationship for the lift curve, accounting for the non-linear nature of the $C_L$ vs. $\alpha$ curve. The expression is

$$C_L = \frac{2\pi A}{P/b+2}\, \alpha + .0925\left(\frac{\alpha}{\tan^{-1}\frac{A}{4}}\right)^2 - .0146\left(\frac{\alpha}{\tan^{-1}\frac{A}{4}}\right) - \left(.529\alpha - .034\right)\sqrt{t/c}$$

This relationship accounts for the formation of the spiral vortex which begins immediately as any lift is developed on the delta. (In other words, linearized potential theory will predict the lift curve only at zero lift.) The correlation of the low Reynolds Number test data with this relationship is good, and it is concluded that it accounts for the combined effects of the primary and secondary vortices.

24

EXAMINATION OF EMPIRICAL DATA

One of the purposes of the investigation reported in this paper was to examine published data to determine what relations exist between wing planform and the low speed aerodynamic characteristics of the wing. Experimental results which were examined were for triangular planforms including delta, double-delta, diamond, arrow, cranked, and various polygon shaped planforms, and "conventional" wings including straight, tapered, sweptback and W-shaped wings. Practically all wings were of aspect ratios from 1.5 to 6.5 (a few exceptions included to assist in curve plotting).

In order to concentrate on planform effect only, section modifications and high-lift devices, such as droopsnoots, leading-edge flaps, slats, spoilers, trailing-edge flaps, suction and blowing boundary control, were not included (again, with exceptions noted later).

It was felt that by amassing all the available data on the high-speed planform wings the gross behavior due to planform would emerge. Accordingly, data for wings was extracted from all reports in sections D (Refs. 88-129) and E (Refs. 130-155) but only from a few references (Refs. 3, 157, 159, 161, 164, 168, 173, 175, 178, 180, 197) in the other sections because of the greater amount of data available. These data include wings ranging from flat-plates to 15% thick, with sharp and with rounded edges, and having airfoils

sections including four-digit series, laminar-flow and double-wedge types. In each case, the data for the "basic wing" was used.

In particular, planform effects on the lift curve, drag-lift ratio, and on the pitching moment derivative were examined and are treated below.

## Lift Curve

The effects of planform on the lift curve ($C_L$ vs. $\alpha$) are difficult to clearly define because they are masked to a great extent by the airfoil section variables. The parameters of interest are:

(1) Angle of zero-lift, $\alpha_{L} = 0$

(2) Lift-curve slope, $\dfrac{dC_L}{d\alpha}$

(3) $C_{L_{max}}$

$\dfrac{dC_L}{d\alpha}$ at $C_L = 0$ is called $C_{L_\alpha}$ in this report. In addition, $\dfrac{dC_L}{d\alpha}$ at $C_L = 0.8$ was examined. $C_L = 0.8$ was chosen because this number is approximately the value of $C_L$ of the present generation of jet transports in the approach configuration. Accordingly, $D/L$ and $\dfrac{dC_M}{dC_L}$ have also been examined at $C_L = 0.8$.

$C_{L_{max}}$ is a joint product of airfoil section and planform. The section variations, particularly leading-edge curvature and the effective camber as produced by flapped

sections, produce the largest increments in $C_{L_{max}}$. The planform effect results from the planform producing a spanwise lift distribution which may be considerably different from the spanwise distribution of section maximum lift distributions. Wing $C_{L_{max}}$ results when local stall is attained. When a large amount of sweepback is involved, the three-dimensional boundary-layer behavior complicates the problem of predicting the position (and $C_L$ magnitude) of first local stall. In addition, large sweepback usually involves the appearance, well below maximum $C_L$, of extremely non-linear pitching-moment curves which usually further limit the usable $C_L$. This aspect of $C_{L_{max}}$ is very well discussed in reference 2.

Figures 12a and 12b show typical effects of section changes and of high-lift devices on a swept-wing and on a delta wing. Because of section effects, such as shown in 12a and 12b, which tend to mask the planform effects, it was particularly difficult to ferret out planform effects on $C_{L_{max}}$.

Figure 13 gives some idea of the effect of aspect ratio in the case of two families of delta wings. At least implied is the conclusion that the best aspect ratio for delta wings is something less than 2.0. Figure 14 confirms this conclusion; the "best" aspect ratio is about 1.87. [For delta wings, $A = \dfrac{2b}{c_r}$.] $A = 1.87$ corresponds to a delta wing having a nose angle of about 50 degrees ($\varepsilon = 25°$, $\Lambda = 65°$).

Figure 15 shows $C_{L_{max}}$ as a function of aspect ratio. Although lines indicating the trend of untapered ($\lambda = 1$) and tapered ($0.2 < \lambda < 1.0$) are shown, the trend does not show significant variation with aspect ratio. The only conclusions which can be reached are that $C_{L_{max}}$ for tapered wings is slightly better than for untapered wings at all aspect ratios, and in the aspect ratio range from 1.4 to 2.4, the delta is the best planform.

Sweepback angle is apparently a more meaningful variable in relation to $C_{L_{max}}$. Figure 16 shows $C_{L_{max}}$ for delta wings as a function of leading edge sweep angle, and the previous conclusion is confirmed: the optimum leading-edge sweepback for a delta wing is about 65 degrees.

Figure 17 shows $C_{L_{max}}$ for wings having non-delta planforms. The apparent trend indicates a slight increase of $C_{L_{max}}$ as sweepback (or sweep-forward) is increased. Delta wings hold a slight superiority in the range of sweepback from 60 to 70 degrees.

Figure 18 shows the variation in $C_{L_{max}}$ for wings with varying sweep along the leading-edge. The broken curves are the values of $C_{L_{max}}$ estimated from reference 134 for two supersonic transport models (A, high aspect ratio model, and B, moderate aspect ratio model). Reference 134 states, "The computation of force and moment coefficients for all wing

sweeps of a given configuration was based on the dimensions corresponding to the total wing area, including fixed wing, at the 75° sweep condition of that particular configuration." This method is proper practice and produces results which truly show the effect of wing sweep (just as coefficients for wings with extended flaps are calculated using the basic wing area).

However, for the purpose of comparing a wing at a given sweep with other wing planforms (as is done in this report), it is necessary to base each coefficient on the particular planform area of each wing. Accordingly, the values of $C_{L_{max}}$ represented by the open symbols have been divided by the ratio $(S/S_{75°})$ producing the shaded symbols and shifting the data from the broken curves to the solid curves.

The curves presented in figure 18 are for the plain wing (cruise configuration -- no slats, flaps, etc.) so that they may be compared with the previous curves. The curves may be misleading; it should not be concluded that, for example, wing B has the best configuration for low-speed flight at A = 4 (about 35° sweepback). The high $C_{L_{max}}$ values at the high sweep angles are accompanied by unfavorable slopes of the pitching moment curves. For a configuration using leading-edge flaps and trailing-edge double-slotted flaps, reference 134 reports usable (that is, pitchstable) $C_{L_{max}}$ values of 2.05 at $\theta$ = 13.5 degrees for wing A.

It has been proposed that, paralleling slender-body lifting theory and highly-loaded wing theory, the correct parameter for comparing wing performance should be $C_L/A$ rather than $C_L$.

$$\frac{C_L}{A} = \frac{L}{qS} \cdot \frac{S}{b^2} = \frac{L}{qb^2}$$

This parameter has the advantage of eliminating wing area so that a shift of curves, as in figure 18, is not necessary. It is interesting to note that when the data from figure 18 is plotted, using $\frac{C_{L_{max}}}{A}$ , the difference between the high aspect ratio and moderate aspect ratio wings disappear. (see Fig. 19). It is logical that only one curve would appear in figure 19, for the difference between wing A and B is due to area only. ("The lift of the slender (planform) airfoil depends only on the width and not on the area." -- Ref. 3) Although in figure 19 $C_L/A$ is plotted as a function of outboard sweep, a plot of $C_{L_{max}}$ / A against aspect ratio would show the same result.

Planform effects on the lift-curve slope have been treated more extensively in the literature than have the effects on $C_{L_{max}}$ . For this reason, the behavior of $C_{L_\alpha}$ is fairly well known. For example, the major parameter affecting $C_{L_\alpha}$ for rectangular wings is the aspect ratio with $C_{L_\alpha}$ decreasing as A decreases. Figure 20 shows this relationship.

For triangular wings and other high-speed wings of low aspect ratio the lift curve may be analyzed using slender wing theory. Jones and Cohen (Ref. 3) point out that $C_L$ for these wings will only be satisfactorily given by this theory for very low aspect ratios (A $\leq$ 1). For higher aspect ratios they present an empirical formula for rectangular and tapered wings. This formula is:

$$C_{L_\alpha} \approx \frac{2\pi A}{57.3\left(\frac{PA}{b} + 2\right)} \qquad \text{(A)}$$

Figure 21 shows the excellent agreement of delta-wing data with this equation; it also shows the satisfactory agreement with $C_L = \frac{\pi A}{2(57.3)}$ up to A = 1.0.

Since lifting-line theory is inadequate to predict the characteristics of wings having appreciable angles of sweep and/or very low aspect ratio, lifting-surface theories have been developed to predict the characteristics of these wings. Most of references 8-58 are involved with these theories or their simplification, extension, or application; most involve an extensive volume of computing labor.

As previously noted, one of the first satisfactory presentations of lifting surface theory was by Weissinger (Ref. 58). A useful explanation and application of it was presented by De Young and Harper (Ref. 20). This simplified lifting-surface theory can be used to predict the characteristics of conventional wings as well as those having swept and/or low aspect ratio planforms. Symmetric span

31

load distributions may be calculated for wings which are symmetrical about the root chord and have a straight quarter-chord line over the semi-span; there may be arbitrary chord distribution, sweep, aspect ratio, and continuous twist.

From the quantity of material published since 1948, extending, explaining, or offering substitute methods, it might appear as though the Weissinger method were inadequate. Figure 21, however, indicates that the Weissinger method gives reasonably good agreement with empirical data for delta-wings. At all points, the variation of the calculated values from the actual values is less than the spread in the measured values. However, it can be seen that the empirical relation (A) cannot be used for delta-wings.

Also plotted on figure 21 are values for parawings (Rogallo-type wings) which have a triangle-shaped planform. Some of these have conical canopies and some have cylindrical canopies. They cannot be considered triangular wings as defined earlier in this report because of the tendency for the flexible canopy to align itself with the wind direction at the leading-edge. It will be noted from figure 21 that the behavior of these wings is considerably different from that of delta wings.

Figure 22 is reproduced from T.R.921 (Ref. 20). It is one of the most complete presentations of $C_{L_\alpha}$ as affected by sweepback and taper. Figure 23 is a similar graph

reproduced from Figure A,7t, reference 3, with additional points added.

As noted earlier in this report most papers consider only one slope, i.e., $C_{L_\alpha} = \frac{dC_L}{d\alpha}$ at $C_L = 0$, whereas it is typical of triangular wings that the slope of the lift-curve is not constant. Close examination of the curves in figure 24 will show that the slope of the curve of the straight wing is constant for most of its length but the slope of the sweptback wing and of the delta wing increases before decreasing as the angle of attack increases. The following values are obtained from the curves in figure 24:

| $\Lambda$ (deg.) | $C_{L_\alpha}$ (per deg.) | Max $\frac{dC_L}{d\alpha}$ (per deg.) |
| --- | --- | --- |
| 0 | .07 | .07 (from $C_L = 0$ to $C_L = .8$) |
| 49.1 | .047 | .069 (at $C_L = .5$) |
| 59 (delta) | .045 | .052 (from $C_L = .6$ to $C_L = .8$) |

Figures 25 and 26 show one examination of this change in slope of the lift curve. The value of $\frac{dC_L}{d\alpha}$ at $C_L = .8$ was recorded for the wings studied in this report. The values for triangular wings were plotted in figure 25 and for swept-back tapered wings in figure 26. Compared with the values of $C_{L_\alpha}$ it will be noted that at lower aspect ratios, the slope at $C_L = .8$ is greater than at $C_L = 0$ and the reverse is true at high aspect ratios. This effect is pronounced for triangular wings (deltas and tapered wings swept 60°).

## Drag Polar

The parameters of interest which can be obtained from a plot of $C_D$ vs. $C_L$ (or of $C_D$ vs. $C_L^2$) are:

(1)   Minimum drag coefficient, $C_{D_o}$

(2)   $C_D$ and D/L at $C_L = 0.8$

(3)   Span efficiency factor, e; where $C_{D_L} = \dfrac{C_L^2}{\pi A e}$ and $\dfrac{dC_D}{dC_L^2} = \dfrac{1}{\pi A e}$

As pointed out by Jones and Cohen the greatest practical consequence of the separation of the vortex surface from the leading-edge is the rapid increase of drag with angle of attack. "After the flow becomes detached from the edge, the forward suction force no longer increases in proportion to the lift, with the result that the theoretical formulas for drag no longer apply and the resultant force on the wing falls back toward a direction at right angles to the chord plane. Prior to the occurance of separation the drag is observed to follow roughly the theoretical minimum value

$$C_D = C_{D_o} + \frac{C_L^2}{\pi A}$$

but at higher angles of attack the value

$$C_D = C_{D_o} + C_L \tan \alpha$$

is approached." -(Ref. 3)

Figure 27 shows this effect for a delta wing of aspect ratio 1.8. It will be noted that the $C_D$ variation agrees very closely with $C_{D_o} + C_L \tan \alpha$ at all angles of attack--

not just at "higher angles." Figure A,8f of reference 3 purports to show a clear relationship between planform and drag due to lift; the actual relationship is not as clear as that figure implies. Figure 28 gives an example of the effect of planform on $C_{D_i}$. The plot of $C_{D_o} + C_L \tan \alpha$ becomes a band rather than a single curve because of the difference in lift-curve slopes for the various wing planforms. The only conclusion which can be reached from figure 28 is that the swept-forward wing has higher drag than the others; there is no significant difference between the other planforms.

The $C_D$ curve will lie between the $C_{D_o} + C_L{}^2/\pi A$ curve and the $C_{D_o} + C_L \tan \alpha$. It is desirable of course, to move the curve toward the former boundary. Another way of considering this point is to consider the span efficiency factor. For the delta wing in figure 27, the value of the slope is:

$$\frac{dC_D}{dC_L{}^2} = \frac{1}{\pi Ae} = .348$$

Thus, e = .508!

Figure 29 shows the effectiveness of working with the leading-edge to improve the efficiency factor (i.e., to shift the drag polar toward the polar for an ideal elliptical wing). These data are from reference 129 by Wick and Graham. They applied skewed plain nose flaps (actually a nose-droop) to a large scale aspect ratio 2 delta wing and fuselage and reported that with the nose flaps deflected, "the flow separation

occurred at $C_L$ of .35 compared to approximately .1 for the plain wing. The maximum drag reduction due to the separation delay was approximately 25 per cent.

Figure 29 shows this drag reduction to be a significant proportion of the gain theoretically possible. At $C_L = 0.8$:

$$C_{D_O} + C_L \tan \alpha \simeq .27$$

$$C_D \; (\delta_f = 0°) = .235$$

$$C_D \; (\delta_f = 40°) = .203$$

$$C_{D_O} + C_L^2/\pi A = .112$$

$$\left[ C_D \; (\delta_f = 0°) \right] - \left[ C_{D_O} + \frac{C_L^2}{\pi A} \right] = .123$$

Thus, 0.123 is maximum possible $C_D$ improvement.

$$\left[ C_D \; (\delta_f = 0) \right] - \left[ C_D \; (\delta_f = 40°) \right] = \Delta C_D = .032$$

Improvement $= \dfrac{.032}{.123} = 26\%$ of the possible $\Delta C_D$.

Figures 30, 31, and 32 show planform effect on D/L at $C_L = .8$. The penalty of triangular wings (delta-wings and $\Lambda = 60°$) is the high value of D/L at low speeds. Conventional wings (e.g., $\Lambda = 0$) have much lower values of D/L. Figure 32 shows the characteristics of the variable sweep type of planform. As expected, the "high aspect ratio" model has lower drag and each model has decreasing D/L as aspect ratio is increased.

Figure 33 compares two delta wings with two double-

deltas. This is new, unpublished data obtained by W. H. Wentz at Wichita State University.

## Bibliography

This bibliography includes the listing of the most valuable of the references consulted during the preparation of this report. In addition to the sources listed, over 200 other reports and papers were examined and discarded as being not applicable. In general, aspect ratios of 2 or more and Mach numbers less than about 0.4 were considered.

An attempt has been made to make this bibliography more useful by classifying the references. The following catagories are used:

A. General Discussions and/or Reviews of the Low-Speed Flight Characteristics of High-Speed Wings

B. Analytical Methods for the Determination of Span Loading and/or the Prediction of the Aerodynamic Characteristics of Various Wing Planforms

C. Descriptions of Flow and Flow Visualization

D. Aerodynamic Characteristics of Delta Wings

E. Characteristics of Various High-Speed Wing Planforms (including Diamond, W-, M-, Arrow, Cranked, Curved-Leading-Edge, and Other Planforms)

F. Effect of Various Leading-Edge Slats, Flaps, or Nose Modifications and of Trailing-Edge High-Lift or Stall-Control Devices on the Characteristics of Swept Wings

G. Swept-Back Wings

H. Variable-Sweep Wings

I. Boundary-Layer Control Applied to a High-Speed Wing

J. Miscellaneous

The papers are arranged alphabetically by authors in each group. In the many cases in which a paper fits in more than one catagory, it was arbitrarily classified in one group only (usually the first group to which it applied; e.g., a paper containing data on delta, diamond, and sweptback wings would fit in groups D, E, and G; it would be classified in D).

38

A. General Discussions and/or Reviews

    1. Abbot, I. H., A. E. von Doenhoff, and L. S. Stivers. "Summary of Airfoil Data," NACA TR 824, 1945.

    2. Harper, C. W. and R. L. Maki. "A Review of the Stall Characteristics of Swept Wings," NASA TN D2373, 1964.

    3. Jones, R. T. and Doris Cohen. "High Speed Wing Theory," Princeton Aeronautical Paperbacks, Princeton Univ. Press, Princeton, N. J., 1960.

    4. von Karman, T. "Some Significant Developments in Aerodynamics Since 1946," JOUR. AERO. SCI., Vol. 26, No. 3, March, 1959.

    5. Schairer, G. S. "Some Opportunities for Progress in Aircraft Performance," JOUR. AIRCRAFT, Vol. 1, No. 2, March-April, 1964.

    6. Thomas, H. H. B. M. "State of the Art of Estimation of Derivatives," AGARD-339, N62-12256.

    7. Wimpress, J. K. and J. M. Swihart. "Influence of Aerodynamic Research on the Performance of Supersonic Airplanes," JOUR. AIRCRAFT, Vol. 1, No. 2, March-April, 1964.

B. Analytical Methods

    8. Adams, M. C. "Leading-Edge Separation from Delta Wing at Supersonic Speeds," JOUR. AERO. SCI., Reader's Forum, Vol. 20, No. 6, June, 1953.

    9. Anderson, R. F. "Determination of the Characteristics of Tapered Wings," NACA TR 572, 1940.

   10. Bergesen, A. and J. D. Porter. "An Investigation of the Flow around Slender Delta Wings with Leading-Edge Separation," Princeton Univ. Press, Princeton, N. J., May, 1960.

   11. Brown, C. E. and W. H. Michael, Jr. "On Slender Delta Wings with Leading-Edge Separation," NACA TN 3430, April, 1955.

   12. Brown, C. E. and W. H. Michael, Jr. "Effect of Leading-Edge Separation on the Lift of a Delta Wing," JOUR. AERO. SCI., Vol. 21, No. 10, October, 1954.

   13. Campbell, G. S. "A Finite-Step Method for the Calculation of Span Loadings of Unusual Planforms," NACA RM L50L13, 1951.

14. Cheng, H. "Remarks on Nonlinear Lift and Vortex Separation," JOUR. AERO. SCI., Reader's Forum, Vol. 21, No. 3, March, 1954.

15. Cohen, D. "A Method for Determining the Camber and Twist of a Surface to Support a Given Distribution of Lift, with Applications to the Load over a Swept-back Wing," NACA TR 826, 1945.

16. Cone, C. D., Jr. "A Theoretical Investigation of Vortex-Sheet Deformation behind a Highly Loaded Wing and Its Effects on Lift," NASA TN D-657, 1961.

17. Cone, C. D., Jr. "The Aerodynamic Design of Wings with Cambered Span Having Minimum Induced Drag," NASA TR-152, 1963.

18. DeYoung, J. "Theoretical Additional Span Loading Characteristics of Wings with Arbitrary Sweep, Aspect Ratio, and Taper Ratio," NACA TN 1491, 1947.

19. DeYoung, J. "Theoretical Symmetric Span Loading due to Flap Deflection for Wings of Arbitrary Plan Form at Subsonic Speeds," NACA TR 1071, 1952.

20. DeYoung, J. and C. W. Harper. "Theoretical Symmetric Span Loading at Subsonic Speeds for Wings Having Arbitrary Planform," NACA TR 921, 1948.

21. Diederich, F. W. and M. Zlotnick. "Calculated Spanwise Lift Distributions and Aerodynamic Influence Coefficients for Swept Wings in Subsonic Flow," NACA TN 3476, Oct., 1955.

22. Diederich, F. W. and M. Zlotnick. "Calculated Spanwise Lift Distributions, Influence Functions, and Influence Coefficients for Unswept Wings in Subsonic Flow," NACA TR 1228, 1955. (Supersedes TN 3014)

23. Edwards, R. H. "On Leading-Edge Separation from Delta Wing," JOUR. AERO. SCI., Vol. 21, No. 2, February, 1954.

24. Falkner, V. M. "The Calculation of the Aerodynamic Loading on Surfaces of Any Shape," Aero. Res. Counc., R & M 1910, 1943.

25. Falkner, V. M. "The Solution of Lifting Plane Problems by Vortex Lattice Theory," Aero. Res. Counc., R & M 2591, 1947.

26. Falkner, V. M. and D. Lehrian. "Calculated Loadings Due to Incidence of a Number of Straight and Swept-Back Wings," Aero. Res. Counc., R & M 2596, 1948.

27. Garner, H. C. "Methods of Approaching an Accurate Three-Dimensional Potential Solution for a Wing," Aero. Res. Counc., R & M 2721, 1948.

28. Graham, D. "A Modification to Thin-Airfoil-Section Theory, Applicable to Arbitrary Airfoil Sections, to Account for the Effects of Thickness on the Lift Distribution," NACA TN 2298, 1951.

29. Holme, O. "The Approximate Solution of the Lifting Surface Problem with the Aid of Discrete Vortices," Royal Inst. Tech., Div. of Aero., Tech Note 6, Stockholm, 1949.

30. Jones, A. L.; O. P. Lamb; and A. E. Cronk. "A Method for Predicting Lift Effectiveness of Spoilers at Subsonic Speeds," JOUR AERO. SCI., Vol. 23, No. 4, April, 1956.

31. Jones, R. T. "Effects of Sweepback on Boundary Layer and Separation," NACA TN 1402, 1947.

32. Jones, R. T. "Subsonic Flow Over Thin Oblique Airfoils at Zero Lift," NACA TR 902, 1948.

33. Jones, W. P. "Theoretical Determination of the Pressure Distribution on a Finite Wing in Steady Motion," Aero. Res. Counc., R & M 2145, 1943.

34. Katzoff, S.; M. Faison; and H. C. DuBose. "Determination of Mean Camber Surfaces for Wings Having Uniform Chordwise Loading and Arbitrary Spanwise Loading in Subsonic Flow," NACA TR 1176, 1954.

35. Küchemann, D. "A Simple Method for Calculating the Span and Chordwise Loadings on Thin Swept Wings," Aero. Quart., Vol. 4, 1953.

36. Küchemann, D. "A Simple Method for Calculating the Span and Chordwise Loadings on Straight and Swept Wings of any Given Aspect Ratio at Subsonic Speeds," Aero. Res. Counc., R & M 2935, 1952.

37. Laporte, O. "Rigorous Solutions for the Spanwise Lift Distribution of a Certain Class of Airfoils," QUART. APPL. MATH., Vol. 2, No. 3, Oct., 1944.

38. Laporte, O. and H. Yoshihara. "A Rigorous Method for Finding the Lift of a Certain Class of Airfoils and Remarks on the Meaning of Schrenk's Approximate Rule," JOUR. AERO. SCI., Vol. 22, No. 11, Nov., 1955.

39. Lawrence, H. R. "The Lift Distribution on Low-Aspect-Ratio Wings at Subsonic Speeds," Cornell Aero. Lab, Rept. No. AF-673-A-1, Rev. Aug., 1950.

40. Lawrence, H. R. "Lift Distribution on Low Aspect Ratio Wings at Subsonic Speeds," JOUR. AERO. SCI., Reader's Forum, Vol. 18, No. 10, Oct., 1951.

41. Lawrence, H. R. "The Aerodynamic Characteristics of Low-Aspect-Ratio Wing-Body Combinations in Steady Subsonic Flow," JOUR. AERO. SCI., Vol. 21, No. 8, 1953.

42. Lomax, H. and M. A. Heaslet. "Linearized Lifting-Surface Theory for Swept-Back Wings with Slender Plan Forms," NACA TN 1992, 1949.

43. Maki, R. L. "The Use of Two-Dimensional Section Data to Estimate the Low-Speed Wing Lift Coefficient at which Section Stall First Appears on a Swept Wing," NACA RM A51E15, 1951.

44. Mangler, K. W. and B. F. R. Spencer. "Some Remarks on Multhopp's Subsonic Lifting Surface Theory," R.A.E. Rept. Aero. 2181, August, 1952.

45. Mangler, K. W. and J. H. B. Smith. "Calculation of the Flow Past a Slender Delta Wing with Leading Edge Separation," PROC. ROY. SOC. Series A, Vol. 251, May 26, 1959.

46. Multhopp, H. "Methods for Calculating the Lift Distribution of Wings (Subsonic Lifting Surface Theory), Aero. Res. Counc., R & M 2884, 1950.

47. Mutterperl, W. "The Calculation of Span Load Distributions on Swept-Back Wings," NACA TN 834, 1941.

48. Sacks, A. H., etal. "Low Speed Aerodynamics of Straight and Swept Wings with Flow Separation," Itek Corp., March 31, 1963.

49. Schneider, W. C. "A Comparison of the Spanwise Loading Calculated by Various Methods with Experimental Loading Obtained on a 45° Sweptback Wing of Aspect Ratio 8.02 at a Reynolds Number of 4.0 x 10$^6$," NACA TR 1208, 1954.

50. Schrenk, O. "A Simple Approximation Method for Obtaining the Spanwise Lift Distribution," NACA TM 948, 1940.

51. Smith, J. H. B. "The Properties of a Thin Conically Cambered Wing According to Slender-Body Theory," Aero. Res. Counc., R & M 3135.

52. Soule, H. A. and R. F. Anderson. "Design Charts Relating to the Stalling of Tapered Wings," NACA TR 703, 1940.

53. Staff, Admiralty Res. Lab, Teddington. "Graphical Solution of Multhopp's Equations for the Lift Distribution of Wings," ATI No. 118649, March, 1951.

54. Thwaites, B. "A Continuous Vortex Line Method for the Calculation of Lift on Wings of Arbitrary Plan Form," Aero. Res. Counc., 12,082, 1949.

55. Toll, T. A. and M. J. Queijo. "Approximate Relations and Charts for Low-Speed Stability Derivatives of Swept Wings," NACA TN 1581, 1948.

56. Weber, J. "Design of Warped Slender Wings with the Attachment Line Along the Leading Edge," R.A.E. Rept. Aero. 2530, Sept., 1957.

57. Weber, J. and G. G. Brebner. "A Simple Estimate of the Profile Drag of Swept Wings," R.A.E. Rept. Aero. 2168, June, 1952.

58. Weissinger, J. "The Lift Distribution on Swept-Back Wings," NACA TM 1120, March, 1947.

C. Description of Flow and Flow Visualization

59. Bergesen, A. J. and J. D. Porter. "An Investigation of the Flow around Slender Delta Wings with Leading Edge Separation," ONR Rept. No. 510, Princeton Univ., May, 1960.

60. Berndt, S. B. "Three Component Measurement and Flow Investigation of Plane Delta Wings at Low Speeds and Zero Yaw," Roy. Inst. Tech., Div. of Aero., TN 4, Stockholm, Sweden, 1949.

61. Black, J. "Flow Studies of the Leading Edge Stall on a Swept-Back Wing at High Incidence," J. RAeS., Vol. 60, No. 541, Jan., 1956.

62. Earnshaw, P. B. "Measurements of Vortex-Breakdown Position at Low Speed on a Series of Sharp-Edged Symmetrical Models," RAE-TR-64047, Nov., 1964.

63.* Eichelbrenner, E. A.; P. Laval; and H. Werle. "Decollement sur une aile Delta Placee sans Incidence dans un Ecoulement Laminaire Incompressible (Separation Over a Delta Wing at Zero Incidence in a Laminar Incompressible Flow)," LA RECHERCHE AERONAUTIQUE, ONERA, May-June, 1959.

64. Elle, B. J. "An Investigation at Low Speed of the Flow Near the Apex of Thin Delta Wings with Sharp Leading-Edges," A.R.C. R & M No. 3176, Jan., 1958.

65. Fink, P. T. "Wind Tunnel Tests on a Slender Delta Wing at High Incidence," 1956.

66. Fink, P. T. and J. Taylor. "Some Low-Speed Experiments with 20 Degree Delta Wings," A.R.C. 17,854, September, 1955.

67. Garner, H. C. and D. W. Bryer. "Experimental Study of Surface Flow and Part-Span Vortex Layers on a Cropped Arrowhead Wing," A.R.C. R & M 3107, April, 1957.

68. Hall, M. G. "On the Vortex Associated with Flow Separation from a Leading Edge of a Slender Wing," A.R.C. 21,117, June, 1959.

69. Hall, M. G. "A Theory for the Core of a Leading-Edge Vortex," JOUR. FLUID MECH., Vol. 2, Part 2, 1961.

70. Jones, J. P. "The Breakdown of Vortices in Separated Flow," U.S.A.A. Rept. No. 140, A.R.C. 22,241, July, 1960.

71. Küchemann, D. "Types of Flow on Swept Wings with Special Reference to Free Boundaries and Vortex Sheets," J. RAeS., Vol. 57, No. 515, November, 1953.

72. Lambourne, N. C. and D. W. Bryer. "Some Measurements in the Vortex Flow Generated by a Sharp Leading Edge Having 65 Degrees Sweep," A.R.C. C.P. No. 477, July, 1959.

73. Lambourne, N. C. and D. W. Bryer. "The Bursting of Leading-Edge Vortices--Some Observations and Discussion of the Phenomenon," A.R.C. R & M No. 3282, London, 1962

74. Lambourne, N. C. and D. W. Bryer. "The Structure of the Vortex Flow Generated by a Sharp Leading Edge Having 65 Degrees Sweep," (to be issued).


*In French; translation available from Aero. Engr. Dept., Wichita State University

75. Lambourne, N. C. and P. S. Pusey. "Some Visual
Observations of the Effects of Sweep on the Low-
Speed Flow Over a Sharp-Edged Plate at Incidence,"
A.R.C. R & M No. 3106, London, January, 1958.

76. Marsden, D. J.; R. W. Simpson; and W. J. Rainbird.
"An Investigation into the Flow Over Delta Wings at
Low Speeds with Leading Edge Separation," A.R.C.
20409, February, 1958.

77. Maskell, E. C. "Flow Separation in Three Dimensions,"
A.R.C. 18,063, November, 1955.

78. Ornberg, T. "A Note on the Flow Around Delta Wings,"
KTH- Aero. TN No. 38, 1954.

79. Owen, T. B. "Techniques of Pressure-Fluctuation
Measurements Employed in the R.A.E. Low-Speed Wind
Tunnels," AGARD Rept. 172, 1958.

80. Peckham, D. H. "Low-Speed Wind-Tunnel Tests on a
Series of Uncambered Slender Pointed Wings with
Sharp Edges," A.R.C. R & M No. 3186, December, 1958.

81.* Persoz, B. and G. Grenier. "Enduits de Visualisation
a Base de Corps Gras," LA RECHERCHE AERONAUTIQUE,
ONERA, No. 60, 1957.

82.* Roy, Maurice. "Sur la Theorie de L'aile en Delta
(On the Theories of the Delta Wing)," LA RECHERCHE
AERONAUTIQUE, ONERA, No. 56, February, 1957.

83. Spreiter, J. R. and A. H. Sacks. "The Rolling Up
of the Trailing Vortex Sheet and Its Effect on the
Downwash Behind Wings," JOUR. AERO. SCI., Vol. 18,
No. 1, January, 1963.

84. Squire, H. B. "Analysis of the 'Vortex Breakdown'
Phenomenon, Part I," Imperial Col. of Sci. and Tech.,
Aero. Dept., Rept. 102, 1960.

85. Titchener, I. M. and A. J. Taylor-Russel. "Experiments
on the Growth of Vortices in Turbulent Flow," A.R.C.
C.P. 316, March, 1956.

86.* Werle, H. "Essai de Verification de la Conicite de
L'ecolement Antour d'une aile Delta Mince avec Incidence
(Verification Test of the Conical Flow Around a Slender
Delta Wing with Incidence)," LA RECHERCHE AERONAUTIQUE,
ONERA, No. 63, 1958.

*In French; translation available from Aero. Engr. Dept.,
Wichita State University

87.* Werle, H.  "Sur L'Eclatement des Tourbillom D'apex D'une Aile Delta aux Faibles Vitesses (On the Explosion of Vortices Above a Delta Wing at Low Speeds)," LA RECHERCHE AERONAUTIQUE, ONERA, No. 74, January-February, 1960.

D.  Delta Wings

88.  Alexander, A. J.  "Low Speed Wind Tunnel Test of 70° Cropped Delta Wing with Edge Blowing," Col. of Aero., Cranfield, Rept. 162.

89.  Anderson, A. E.  "An Investigation at Low-Speed of a Large Scale Triangular Wing of $AR = 2$ Characteristics of a Wing Having a Double Wedge Airfoil Section with Maximum Thickness at 20% C," NACA RM A7F06, Nov., 1947.

90.  Anderson, A. E.  "An Investigation at Low Speed of a Large-Scale Triangular Wing of Aspect Ratio Two.  II - The Effect of Airfoil Section Modifications and the Determination of the Wake Downwash," NACA RM A7H28, 1947.

91.  Anderson, A. E.  "Chordwise and Spanwise Loadings Measured at Low Speed on Large Triangular Wings," NACA RM A9B17, 1949.

92.  Anderson, A. E.  "An Investigation at Low Speed of a Large Scale Triangular Wing of $AR= 2$ - III Characteristics of Wings with Body and Vertical Tail," NACA RM A9H04, Oct., 1949.

93.  Berndt, S. B. and K. Orlik-Rückemann.  "Comparisons Between Theoretical and Experimental Lift Distributions of Plane Delta Wings at Low Speeds and Zero Yaw," Royal Inst. Tech., Div. of Aero., TN 10, Stockholm, Sweden, 1949.

94.  Boyd, J. W.; E. Migotsky; and B. E. Wetzel.  "A Study of Conical Camber for Triangular and Sweptback Wings," NACA RM A55G19, Nov., 1955.

95.  Bugg, F. M.  "Effects of Aspect Ratio and Canopy Shape on Low-Speed Aerodynamic Characteristics of 50° Swept Parawings," NASA TN D-2922, July, 1965.

96.  Cone, C. D., Jr.  "Low-Speed Static Longitudinal and Lateral Stability Characteristics of a Variable-Incidence Delta-Wing Canard Model with High-Lift Canard Surfaces," NASA TM X-72, Sept., 1959.

*In French; translation available from Aero. Engr. Dept., Wichita State University

97. Croom, D. R. "Characteristics of Flap-Type Spoiler Ailerons at Various Locations on a 60° Delta Wing with a Double Slotted Flap," NACA RM L52J24, Dec., 1952.

98. Dods, J. B., Jr. "Control Effectiveness and Hinge-Moment Characteristics at Low Speed of Large-Chord, Horn-Balanced, Flap-Type Controls on a Triangular Wing of Aspect Ratio 2," NACA RM A52F13, Aug., 1952.

99. Franks, R. W. "Tests in the Ames 40- by 80- Foot Wind Tunnel of an Airplane Model with an Aspect Ratio 4 Triangular Wing and an All-Movable Horizontal Tail-High-Lift Devices and Lateral Controls," NACA RM A52K13, Feb., 1953.

100. Furlong and McHugh. "A Summary and Analysis of the Low-Speed Longitudinal Characteristics of Swept Wings at High Reynolds No.," NACA Rept. 1339, 1957.

101. Graham, D. "Chordwise and Spanwise Loadings Measured at Low Speeds on a Large Triangular Wing Having an Aspect Ratio of 2 and a Thin, Subsonic-Type Airfoil Section, NACA RM A50A04a, 1950.

102. Graham, D. "The Low-Speed Lift and Drag Characteristics of a Series of Airplane Models Having Triangular or Modified Triangular Wings," NACA RM A53D14, June, 1953.

103. Graham, D. and D. G. Koenig. "Tests in the Ames 40- by 80-Foot Wind Tunnel of an Airplane Configuration with an Aspect Ratio 2 Triangular Wing and an All-Movable Horizontal Tail-Longitudinal Characteristics," NACA RM A51B21, April 23, 1951.

104. Graham, D. and D. G. Koenig. "Tests in the Ames 40- by 80-Foot Wind Tunnel of an Airplane Configuration with an Aspect Ratio 4 Triangular Wing and an All-Movable Horizontal Tail - Longitudinal Characteristics," NACA RM A51H10a, Oct., 1951.

105. Henderson, W. P. "Longitudinal Stability Characteristics of Low-Aspect-Ratio Wings Having Variations in Leading- and Trailing-Edge Contours," NASA TN D-1796, Oct., 1964.

106. Holmbe, V. "The Center of Pressure Position at Low Speeds and Small Angles of Attack for a Certain Type of Delta Wings," SAAB TN 13, Linkölping, Sweden, 1953.

107. Jaquet, B. M.  "Effects of Horizontal-Tail Position, Area, and Aspect Ratio on Low-Speed Static Longitudinal Stability and Control Characteristics of a 60° Triangular-Wing Model Having Various Triangular-All-Movable Horizontal Tails," NACA RM L51I06, Dec., 1951.

108. James, J. A. and L. W. Hunton.  "Estimation of Incremental Pitching Moments Due to Trailing-Edge Flaps on Swept and Triangular Wings," NACA TN 4040, July, 1957.

109. Jaszlics, I. and L. Trilling.  "An Experimental Study of the Flow Field About Swept and Delta Wings with Sharp Leading Edges," JOUR. A/S SCI., Vol. 26, No. 8, August, 1959.

110. Kelly, M. W. and J. Tolhurst.  "The Use of Area Suction to Increase the Effectiveness of a Trailing-Edge Flap on a Triangular Wing of $AR = 2$, " NACA RM A54A25, April, 1954.

111. Koenig, D. G.  "Tests in the Ames 40- by 80-Foot Wind Tunnel of an Airplane Configuration with an Aspect Ratio 3 Triangular Wing and an All-Movable Horizontal Tail-Longitudinal and Lateral Characteristics," NACA RM A52L15, April, 1953.

112. Koenig, D. G.  "Tests in the Ames 40- by 80-Foot Wind Tunnel of an Airplane Configuration with a Variable Incidence Triangular Wing and an All-Movable Horizontal Tail," NACA RM A53D21, June, 1953.

113. Koenig, D. G.  "Tests in the Ames 40- by 80-Foot Wind Tunnel of the Effects of Various Wing Modifications on the Long Characteristics of Two-Triangular Wing Airplane Models with and without Horizontal Tails," NACA RM A54B09, April, 1954.

114. Koenig, D. G. and V. R. Corsiglia.  "Large Scale Wind Tunnel Tests on an Aspect Ratio 2.17 Delta-Wing Model Equipped with Mid Chord Boundary-Layer-Control Flaps," NASA TN D-2552, Dec., 1964.

115. Lange, and Wacke.  "Pruefbericht uber 3- and 6-Komponenten-messungen an der Zuspitzungsreihe von Flegeln kleiner Streckung (Test Report on Three- and Six-Component Measurements on a Series of Tapered Wings of Small Aspect Ratio (Partial Report:  Triangular Wing)," Translated as NACA TM 1176, May, 1948.

116. Lawford, J. A. and A. R. Beauchamp. "Low-Speed Wind
     Tunnel Tests on a Thin Sharp-Edged Delta Wing with
     70° Leading-Edge Sweep with Particular Reference to
     the Position of Leading-Edge Vortex Breakdown,"
     Aero. Res. Counc., R & M 3338.

117. Lichtenstein, J. H. and B. M. Jaquet. "Low-Speed
     Static Longitudinal Stability and Control Character-
     istics of 60° Triangular-Wing and Modified 60°
     Triangular-Wing Models Having Half-Delta and Half-
     Diamond Tip Controls," NACA RM L51K08, Feb., 1952.

118. Palmer, W. E. "Effect of Reduction in Thickness from
     6 to 2 Per Cent and Removal of the Pointed Tips on
     the Subsonic Static Longitudinal Stability Character-
     istics of a 60° Triangular Wing in Combination with a
     Fuselage," NACA RM L53F24, Aug., 1952.

119. Powers, B. G. and N. W. Matheny. "Flight Evaluation
     of Three Techniques of Demonstrating the Minimum
     Flying Speed of a Delta-Wing Airplane," NASA TN D-2337,
     July, 1964.

120. Riebe, J. M. and J. C. Graven. "Low Speed Investigation
     of the Effects of Location of a Delta and Straight Tail
     on the Longitudinal Stability and Control of a Thin
     Delta Wing with Extended Double Slotted Flaps," NACA
     RM L53J26, Jan., 1954.

121. Rose, L. M. "Low-Speed Investigation of a Small
     Triangular Wing of Aspect Ratio 2.0. I – The Effect
     of Combination with a Body of Revolution and Height
     Above the Ground Plane," NACA RM A7K03, Aug. 27, 1948.

122. Rose, L. M. "Low-Speed Investigation of a Small
     Triangular Wings of AR 2.0  II – Flaps, NACA RM A7L11,
     Aug., 1948.

123. Smith, D. W. and V. D. Reed. "A Comparison of the
     Chordwise Pressure Distribution and Spanwise Distribution
     of Loading at Subsonic Speeds on Two Triangular Wings
     of Aspect Ratio Two Having NACA 0005 and 0008 Sections,"
     NACA RM A51L21, May, 1952.

124. Ware, G. M. "Low-Subsonic Aerodynamic Characteristics
     of a Delta Wing Recovery Device for Nonlifting Space-
     craft," NASA TN D-2349.

125. Weirich, R. L. "Analytic Determination of the Take-Off
     Performance of Some Representative Supersonic Transport
     Configurations," NASA, Langley Station, Interim draft
     L-3386.

126. Wentz, W. H. Report to be published on tests con-
ducted on delta and double-delta wings in the 7x10
wind tunnel at Wichita State University, 1965.

127. Wentz, W. H. "A Proposal to Investigate the Flow
Fields About Delta and Double-Delta Wings at Low
Speeds, Phase 2," Aero. Engr. Dept., Wichita State
University, July, 1965.

128. Wick, B. H. "Chordwise and Spanwise Loadings Measured
at Low Speed on a Triangular Wing Having an Aspect
Ratio of Two and an NACA 0012 Airfoil Section," NACA
TN 1650, 1948.

129. Wick, B. H. and D. Graham. "Exploratory Investigation
of the Effect of Skewed Plain Nose Flaps on the Low-
Speed Characteristics of a Large Scale Triangular
Wing Fuselage Model," NACA RM A9K22, Jan., 1950.

E.  Other High Speed Planforms

130. Alford, W. J., Jr. and W. P. Henderson. "An Exploratory
Investigation of the Low-Speed Aerodynamic Character-
istics of Variable-Wing-Sweep Airplane Configurations,"
NASA TM X-142, 1959.

131. Barnett, U. R., Jr. and R. H. Lange. "Low-Speed
Pressure-Distribution Measurements at a Reynolds
Number of $3.5 \times 10^6$ on a Wing with Leading-Edge
Sweepback Decreasing from 45° at the Root to 20° at
the Tip," NACA RM L50A23a, 1950.

132. Bartlett, G. E. and R. J. Vidal. "Experimental Investi-
gation of Influence of Edge Shape on the Aerodynamic
Characteristics of Low Aspect Ratio Wings at Low Speeds,"
JOUR. AERO. SCI., Aug., 1955.

133. Brown, A. E. "Low-Speed Wind-Tunnel Results for a
Thin AR = 1.85 Pointed-Wing-Fuselage Model with Double
Slotted Flaps," NACA RM L56D03, July, 1956.

134. Cook, A. M.; R. K. Greif; and K. Aoyagi. "Large-Scale
Wind Tunnel Investigation of the Low-Speed Aerodynamic
Characteristics of a Supersonic Transport Model Having
Variable-Sweep Wings," NASA TN D-2824.

135. Flax, A. H. and H. R. Lawrence. "The Aerodynamics of
Low-Aspect-Ratio Wings and Wing-Body Combinations,"
Third Anglo-American Aero. Conf., 1951.

136. Flight Sciences Group, N.A.A. Inter-Office Ltr.
"Simple Methods for Preliminary Evaluation of Static
Longitudinal Characteristics of Irregular Planforms,"
North American Aviation, Inc., Los Angeles Div.,
FS-62-7-16, Dept. 282, July 27, 1962.

138. Hayes, W. C. and W. C. Sleeman. "Low-Speed Longitudinal Static Stability and Control Characteristics of Aircraft with Swept Wings and Tail Surfaces Outboard of Wing Tips," NASA Memo 6-11-59L.

139. Henry, B. Z., Jr. "High-Speed Wind-Tunnel Investigation of a Sweptback Wing with an Added Triangular Area at the Center," NACA RM L8J12, Jan., 1949.

140. Holdaway, G. H. and J. A. Mellenthin. "Investigation at Mach Numbers of 0.20 to 3.50 of Blended Wing Body Combinations of Sonic Design with Diamond, Delta, and Arrow Planforms," NASA TM X-372, Aug., 1960.

141. Hopkins, E. J. "Some Effects of Planform Modification on the Skin Friction Drag," NASA RP-170.

142. Lange, R. H. "Maximum-Lift Characteristics of a Wing with the Leading Sweepback Decreasing from 45° at the Root to 20° at the Tip at R. N. from 2.4 to 6.0 x $10^6$," NACA RM L50A04a, July, 1950.

143. Lawrence, H. R. "The Lift Distribution on Low-Aspect-Ratio Wings at Subsonic Speeds," Cornell Aero. Lab, Rept. No. AF-673-A-1, Rev. Aug., 1950.

144. Lowry, J. G. and J. F. Cahill. "Review of the Maximum-Lift Characteristics of Thin and Swept Wings," NACA RM L51E03, June 5, 1951.

145. Malavard, L.; R. Daguenne; M. Enselme and C. Grandjean. "Properties of Sweptback and Delta Wings. Calculations by Electrical Analogy," O.N.E.R.A. Tech. Note No. 25.

146. McCormack, G. M. and V. I. Stevens, Jr. "An Investigation of the Low-Speed Stability and Control Characteristics of Swept-Forward and Swept-Back Wings in the Ames 40- by 80-Foot Wind Tunnel," NACA RM A6K15, 1947.

147. Polhamus, E. C. and R. E. Becht. "Low-Speed Stability Characteristics of a Complete Model with a Wing of W Planform," NACA RM L52A25, April 23, 1952.

148. Purser, P. E. and M. L. Spearman. "Wind-Tunnel Tests at Low Speed of Swept and Yawed Wings Having Various Planforms," NASA TN 2445, Dec., 1951.

149. Smith, D. W. and V. D. Reed. "Subsonic Static Longi-
     tudinal, Stability and Control Characteristics of a
     Wing-Body Combination Having a Pointed Wing of Æ = 2
     with Constant Per Cent Chord T. E. Elevons," NACA
     RM A53C20, May, 1953.

150. Toll, T. A. "Longitudinal Characteristics of Wings,"
     NACA RM L53I21b, Oct., 1953.

151. Tosti, L. P. "Low Speed Static Stability and Damping-
     in-Roll Characteristics of Some Swept and Unswept Low
     Aspect Ratio Wings," NACA TN 1468, Oct., 1947.

152. Treon, S. L. "The Effects of Wing Plan Form on the
     Static Longitudinal Aerodynamic Characteristics of a
     Flat-Top Hypersonic Aircraft at Mach Numbers from 0.6
     to 1.4," NASA TM X-364.

153. Wakefield, R. M. "Effects of Wing-Crank, Leading-Edge
     Chord Extensions and Horizontal-Tail Height on the
     Longitudinal Stability of Swept-Wing Models at Mach
     Numbers from 0.6 to 1.4," NASA TM X-92.

154. Wilson, H. A., Jr. and L. K. Loftin, Jr., "Landing
     Characteristics of High-Speed Wings," NACA RM L8A28e,
     Sept. 21, 1948.

155. Wolhart, W. D. "Static Longitudinal Stability Character-
     istics of a Composite-Planform Wing Model Including
     Some Comparisons with a 45° Sweptback Wing at Transonic
     Speeds," NACA RM L54F24.

F. High-Lift and Stall Control Devices on Swept-Wings

156. Anderson, S. B.; F. H. Matteson; and R. D. Van Dyke, Jr.
     "A Flight Investigation of the Effect of Leading-Edge
     Camber on the Aerodynamic Characteristics of a Swept-
     Wing Airplane," NACA RM A52L16a, Feb., 1953.

157. Barnett, V. R. and S. Lipson. "Effects of Several
     High-Lift and Stall Control Devices on the Aerodynamic
     Characteristics of a Semispan 49° Sweptback Wing,"
     NACA RM L52D17a, Sept., 1952.

158. Bollech, T. V. and G. L. Pratt. "Investigation of Low-
     Speed Aileron Control Characteristics at a Reynolds
     Number of 6.8 x 10$^6$ of a Wing with Leading Edge Swept
     Back 42° with and without High-Lift Devices," NACA
     RM L9E24.

159. Boltz, F. W. and H. H. Shibata. "Pressure Distribution at Mach Numbers up to 0.90 on a Cambered and Twisted Wing Having 40° of Sweepback and an Aspect Ratio of 10, Including the Effects of Fences," NACA RM A52K20, March, 1953.

160. Cahill, J. F. "Comparison of Semi-Span Data Obtained in the Langley Two-Dimensional LTP Tunnel and Full Span Data Obtained in the Langley 19 Foot Pressure Tunnel for a Wing with 40° Sweptback of the .27 Chordline," NACA RM L9B25a, April, 1949.

161. Cahill, J. F. and S. M. Gottlieb. "Low-Speed Aerodynamic Characteristics of a Series of Swept Wings Having NACA 65A006 Airfoil Sections (revised)," NACA RM L50F16, 1950.

162. Conner, D. W. and G. V. Foster. "Investigation of Pressure Distribution Over an Extended Leading Edge Flap on a 42° Sweptback Wing," NACA RM L7J03, Dec., 1947.

163. Evans, W. T. "Data From Large-Scale Low-Speed Test of Airplane Configurations with a Thin 45° Swept Wing Incorporating Several Leading-Edge Contour Modifications," NACA RM A56B17.

164. Foster, G. V. "Effects of Twist and Camber, Fences, and Horizontal-Tail Height on the Low-Speed Longitudinal Stability Characteristics of a Wing-Fuselage Combination with a 45° Sweptback Wing of Aspect Ratio 8 at a Reynolds Number of $4.0 \times 10^6$," NACA RM L52J03, Dec., 1952.

165. Foster, G. V. "Longitudinal Stability and Wake-Flow Characteristics of a Twisted and Cambered Wing-Fuselage Combination of 45° Sweepback and Aspect Ratio 8 with a Horizontal Tail and Stall-Control Devices at a Reynolds Number of $4.0 \times 10^6$," NACA RM L53D08, June, 1953.

166. Foster, G. V. "Effects of Leading-Edge Radius on the Longitudinal Stability of Two 45° Sweptback Wings Incorporating Leading-Edge Camber as Influenced by Reynolds Numbers up to $8.00 \times 10^6$ and Mach Numbers up to 0.290," NACA RM L55H04, Oct., 1955.

167. Foster, G. V. and J. E. Fitzpatrick. "Longitudinal-Stability Investigation of High-Lift and Stall-Control Devices on a 52° Sweptback Wing with and without Fuselage and Horizontal Tail at a Reynolds Number of $6.8 \times 10^6$," NACA RM L8I08, Dec., 20, 1948.

168.   Griner, R. F. and G. V. Foster.   "Low-Speed Longitudinal
       and Wake Air Flow Characteristics at a Reynolds Number
       of 6.0 x 10$^6$ of a 52° Sweptback Wing Equipped with
       Various Spans of Leading Edge and Trailing-Edge Flaps,
       a Fuselage, and a Horizontal Tail at Various Vertical
       Positions," NACA RM L50K29, Feb. 28, 1951.

169.   Guryansky, E. R. and S. Lipson.   "Effect of High-Lift
       Devices on the Longitudinal and Lateral Characteristics
       of a 45° Swept-Back Wing with·Symmetrical Arc Sections,"
       NACA RM L8D06.

170.   Harper, J. J.   "Investigation at Low-Speed at 45° and
       60° Sweptback, Tapered, Low-Drag Wings Equipped with
       Various Types of Full Span, Trailing-Edge Flaps," NACA
       TN 2468, Oct., 1951.

171.   Hopkins, E. J.   "A Wind-Tunnel Investigation at Low
       Speed of Various Lateral Controls on a 45° Swept Model,"
       NACA RM A7L16, April, 1948.

172.   James, H. A.   "Low-Speed Aerodynamic Characteristics
       of a Large Scale 45° Swept-Back Wing with Partial-Span
       Slats, Double-Slotted Flaps, and Ailerons," NACA RM
       A52B19, April, 1952.

173.   James, H. A. and J. K. Dew.   "Effects of Double-
       Slotted Flaps and Leading-Edge Modifications on the
       Low-Speed Characteristics of a Large Scale 45° Swept-
       Back Wing with and without Camber and Twist," NACA
       RM A51D18, July, 1951.

174.   Kelly, J. A. and N. F. Hayter.   "Aerodynamic Character-
       istics of a Leading-Edge Slat on a 35° Swept-Back Wing
       for Mach Numbers from 0.30 to 0.88," NACA RM A51H23,
       Dec., 1951.

175.   Koven, W. and R. R. Graham.   "Wind-Tunnel Investigation
       of High-Lift and Stall-Control Devices on a 37° Swept-
       back Wing of Aspect Ratio 6 at High Reynolds Numbers,"
       NACA RM L8D29, 1948.

176.   Küchemann, D. and D. J. Kettle.   "The Effect of Endplates
       on Swept Wings," R.A.E. Rept. Aero. 2429.

177.   Lacaine, J.   "Characteristics at Landing Speeds of
       60° Sweptback Wings with Trailing-Edge High-Lift
       Devices," LA RECHERCHE AERONAUTIQUE, O.N.E.R.A.

178. Lipson, S. and V. R. Barnett. "Force and Pressure Investigation at Large Scale of a 49° Sweptback Semispan Wing Having NACA 65 A0006 Sections and Equipped with Various Slot Arrangements," NACA RM L51K26.

179. Lowry, J. G. and E. Polhamus. "A Method for Predicting Lift Increments Due to Flap Deflection at Low Angles of Attack in Incompressible Flow," NACA TN 3911, 1957.

180. Maki, R. L. "Full-Scale Wind-Tunnel Investigation of the Effects of Wing Modifications and Horizontal-Tail Location on the Low-Speed Static Longitudinal Characteristics of a 35° Swept-Wing Airplane," NACA RM A52B05, April, 1952.

181. Naeseth, R. L. "Low-Speed Longitudinal Aerodynamic Characteristics of a 45° Sweptback Wing with Double Slotted Flaps," NACA RM L56A10, April, 1956.

182. Naeseth, R. L. "Effect of a Fuselage on the Low-Speed Longitudinal Aerodynamic Characteristics of a 45° Sweptback Wing with Double Slotted Flaps," NACA RM L56G02, Sept., 1956.

183. Naeseth, R. L. and E. E. Davenport. "Investigation of Double Slotted Flaps on a Swept-Wing Transport Model," NASA TN D-103, Oct., 1959.

184. Neely, R. H. and D. W. Conner. "Aerodynamic Characteristics of a 42° Swept-Back Wing with Aspect Ratio 4 and NACA 641-112 Airfoil Sections at Reynolds Numbers from 1,700,000 to 9,500,000," NACA RM L7D14, 1947.

185. Pasamanick, J. and T. B. Sellers. "Low-Speed Investigation of the Effect of Several Flap and Spoiler Ailerons on the Lateral Characteristics of a 47.5° Sweptback-Wing-Fuselage Combination at a Reynolds Number of $4.4 \times 10^6$," NACA RM L50J20, Dec. 8, 1950.

186. Pratt, G. L. and T. V. Bollech. "The Effect of Span and Deflection of Split Flaps and Leading-Edge Roughness on the Longitudinal Stability and Gliding Characteristics of a 42° Sweptback Wing Equipped with Leading-Edge Flaps," NACA RM L9E02.

187. Pratt, G. L. and E. R. Shields. "Low-Speed Longitudinal Characteristics of a 45° Sweptback Wing of Aspect Ratio 8 with High-Lift and Stall-Control Devices at Reynolds Numbers from 1,500,000 to 4,800,000," NACA RM L51J04, 1952.

188. Queijo, M. J.; B. M. Jaquet; and W. D. Wolhart. "Wind-Tunnel Investigation at Low Speed of the Effects of Chordwise Wing Fences and Horizontal-Tail Position on the Static Longitudinal Stability Characteristics of an Airplane Model with a 35° Sweptback Wing," NACA 1203, 1954.

189. Queijo, M. J. and W. D. Wolhart. "Experimental Investigation of the Effect of Vertical-Tail Size and Length and of Fuselage Shape and Length on the Static Lateral Stability Characteristics of a Model with 45° Sweptback Wing and Tail Surfaces," NACA TR 1049, 1951.

190. Racisz, S. F. "Wind-Tunnel Investigation at High and Low Subsonic Mach Numbers of Two Unswept Wings Having NACA 2-006 and NACA 65A006 Airfoil Sections," NACA RM L53J29, Dec., 1953.

191. Salmi, R. J. "Pressure-Distribution Measurements Over an Extensible Leading-Edge Flap on Two Wings Having Leading-Edge Sweep of 42° and 52°," NACA RM L9A18, 1949.

192. Salmi, R. J. "Effects of Leading-Edge Devices and Trailing-Edge Flaps on Longitudinal Characteristics of Two 47.7° Sweptback Wings of Aspect Ratios 5.1 and 6.0 at a R.N. of 6 x $10^6$," NACA RM L50F20.

193. Salmi, R. J. "Low-Speed Longitudinal Aerodynamic Characteristics of a Twisted and Cambered Wing at 45° Sweepback and ÆR 8 with and without High Lift and Stall Control Devices and a Fuselage at R.N. from 1.5 to 4.8 x $10^6$," NACA RM L52C11, June, 1952.

194. Scallion, W. I. "Full-Scale Wind-Tunnel Tests of a 35° Swept-Wing Fighter Airplane with a Spoiler-Slot-Deflector Lateral Control System," NACA RM L56D18.

195. Schneider, W. C. "Effects of Leading-Edge Radius on the Longitudinal Stability Characteristics of Two 60° Sweptback Wings at High Reynolds Numbers," NACA RM L55L30, March, 1956.

196. Schneiter, L. E. and J. M. Watson. "Wind Tunnel Investigation at Low Speeds of Various Plug-Aileron and Lift Flap Configuration on a 42° Sweptback Semi-Span Wing," NACA RM L8K19, Jan., 1949.

197. Spooner, S. H. and E. F. Mollenberg. "Low-Speed Investigation of Several Types of Split Flap on a 47.7° Sweptback Wing-Fuselage Combination of ÆR = 5.1 at a R.N. 6.0 x $10^6$," NACA RM L51D20, July, 1951.

198. Whittle, E. F. and S. Lipson. "Low-Speed, Large-Scale Investigation of Aerodynamic Characteristics of a Semi-Span 49° Sweptback Wing with a Fowler Flap in Combination with a Plain Flap, Slats, and Fences," NACA RM L53D09.

G. Swept-Back Wings

199. Alford, W. J., Jr. and T. J. King, Jr. "Experimental Investigation of Flow Fields at Zero Sideslip Near Swept- and Unswept-Wing-Fuselage Combinations at Low Speed," NACA RM L56J19, Jan., 1957.

200. Anon., Royal Aero. Soc. Data Sheets, Wing, 01.01.01, S01.03.03, S.01.03.04, S.01.03.05, S.01.03.06.

201. Axelson, J. A. and J. F. Haacker. "Subsonic Wing Loadings on a 45° Sweptback-Wing and Body Combination at High Angles of Attack," NASA Memo. 1-18-59A, Feb., 1959.

202. Boltz, F. W.; G. C. Kenyon; and C. O. Allen. "Effects of Sweep Angle on the Boundary-Layer Stability Characteristics of an Untapered Wing at Low Speeds," NASA TN D-338, Oct., 1960.

203. Boltz, F. W. and C. D. Kolbe. "The Forces and Pressure Distribution at Subsonic Speeds on a Cambered and Twisted Wing Having 45° Sweepback, AR= 3 and $\lambda$ of .5," NACA RM A52D22, July, 1952.

204. Cohen, D. "A Method for Determining the Camber and Twist of a Surface to Support a Given Distribution of Lift, with Applications to the Load Over a Sweptback Wings," NACA TR 826.

205. Conard, R. M. "Effects of Sweep in Aircraft Wings Part I - Aerodynamics of Swept Wings at Low Speeds," LA RECHERCHE AERONAUTIQUE, No. 3, 1948-1949.

206. Evans, W. T. "Leading-Edge Contours for Thin Swept Wings: An Analysis of Low- and High-Speed Data," NACA RM A57B11, March, 1957.

207. Faye Petersen, R. "Investigation of Boundary-Layer Flow Over a Swept Wing," M.S. Thesis, Univ. of Wichita, 1953.

208. Foster, G. V. and R. F. Griner. "Low-Speed Longitudinal and Wake Air-Flow Characteristics at a Reynolds Number of 5.5 x $10^6$ of a Circular-Arc 52° Sweptback Wing with a Fuselage and a Horizontal Tail at Various Vertical Positions," NACA RM L51C30, June 19, 1951.

209.  Furlong, G. C. and T. V. Bollech. "Downwash Sidewash and Wake Surveys Behind a 42° Sweptback Wing at a Reynolds Number of 6.8 x 10$^6$ with and without a Simulated Ground," NACA RM L8G22, 1948.

210.  Graham, R. R. "Low-Speed Characteristics of a 45° Sweptback Wing of Aspect Ratio 8 from Pressure Distributions and Force Tests at Reynolds Numbers from 1,500,000 to 4,800,000," NACA RM L51H13, 1951.

211.  Hadaway, W. M. and P. A. Canero. "Low-Speed Longitudinal Characteristics of Two-Unswept Wings of Hexagonal Airfoil Sections Having $AR = 2.5$ and 4 with Fuselage and Horizontal Tail Locations at Various Vertical Locations," NACA RM L53H14a, Feb., 1953.

212.  Hanson, F. H. and R. E. Dannenberg. "Effect of a Nacelle on the Low-Speed Aero Characteristics of a Sweptback Wing," NACA RM A8E12, July, 1948.

213.  Johnson, B. J., Jr. and H. H. Shibata. "Characteristics Throughout the Subsonic Speed Range of a Plane Wing and of a Cambered and Twisted Wing, both Having 45° of Sweepback," NACA RM A51D27, July, 1951.

214.  Koenig, D. G. "Low-Speed Tests of Semispan-Wing Models at Angles of Attack From 0° to 180°," NASA Memo 2-27-59A, April, 1959.

215.  Martina, A. P. "The Interference Effects of a Body on the Spanwise Load Distributions of Two 45° Sweptback Wings of Aspect Ratio 8.02 from Low-Speed Tests," NACA TN 3730, Aug., 1956.

216.  McCormack, G. M. and W. C. Walling. "Aerodynamic Study of a Wing-Fuselage Combination Employing a Wing Sweptback 63° Investigation of a Large Scale Model at Low Speed," NACA RM A8D02, Jan., 1949.

217.  Mirels, H. "Aerodynamics of Slender Wings and Wing-Body Combinations Having Swept Trailing Edges," NACA TN 3105, 1954.

218.  Racisz, S. F. and N. J. Paradiso. "Wind-Tunnel Investigation at High and Low Subsonic Mach Numbers of a Thin Swept-Back Wing Having an Airfoil Section Designed for High Maximum Lift," NACA RM L51L04, Feb., 1952.

219. Salmi, R. J. and W. A. Jacques. "Effect of Vertical Location of a Horizontal Tail on the Static Longitudinal Stability Characteristics of a 45° Sweptback-Wing-Fuselage Combination of Aspect Ratio 8 at a Reynolds Number of 4 x $10^6$," NACA RM L51J08.

220. Schneider, W. C. "Effects of Reynolds Number and Leading-Edge Shape on the Low-Speed Longitudinal Stability of a 6-Per Cent Thick 45° Sweptback Wing," NACA RM L56B14, April, 1956.

221. Shibata, H. H.; A. Bandettini; and J. Cleary. "An Investigation Throughout the Subsonic Speed Range of a Full-Span and a Semispan Model of a Plane Wing and of a Cambered and Twisted Wing, All Having 45° of Sweepback," NACA RM A52D01, June, 1952.

222. Shortal, J. A. and B. Maggin. "Effect of Sweepback and Aspect RAtio on Longitudinal Stability Characteristics of Wings at Low Speeds," NACA TN 1093, 1946.

223. Soule, H. A. "Influence of Large Amounts of Wing Sweep on Stability and Control Problems of Aircraft," NACA TN 1088, June, 1946.

224. Spearman, M. L. and P. Comisarow. "An Investigation of the Low-Speed Static Stability Characteristics of Complete Models Having Sweptback and Swept Forward Wings," NACA RM L8H31, Nov. 19, 1948.

225. Tambor, R. "Flight Investigation of the Lift and Drag Characteristics of a Swept-Wing, Multijet, Transport-Type Airplane," NASA TN D-30, Nov., 1959.

226. Tinling, B. E. and J. K. Dickson. "Tests of a Model Horizontal Tail of Aspect Ratio 4.5 in the Ames 12-Foot Pressure Wind Tunnel. I - Quarter-Chord Line Swept Back 35°," NACA RM A9G13, 1949.

227. Tinling, B. E. and J. K. Dickson. "Tests of a Model Horizontal Tail of Aspect Ratio 4.5 in the Ames 12-Foot Pressure Wind Tunnel. II - Elevator Hinge Line Normal to the Plane of Symmetry," NACA RM A9H11a, 1949.

228. Turner, T. R. "Maximum-Lift Investigation at Mach Numbers from 0.05 to 1.20 of a Wing with Leading Edge Swept Back 42°," NACA RM L9K03, Feb. 14, 1950.

H.  Variable Sweep Wings

229.  Becht, R. E. and A. L. Byrnes, Jr.  "Investigation
      of the Low-Speed Aerodynamic Characteristics of a
      Variable-Sweep Airplane Model with a Wing Having
      Partial-Span Cambered-Leading-Edge Modifications,"
      NACA RM L52G08a, Sept., 1952.

230.  Becht, R. E.  "Stability Characteristics at Low
      Speed of a Variable-Sweep Airplane Model Having
      a Partially Cambered Wing with Several Chord-
      Extension Configurations," NACA RM L53L14, Feb.,
      1954.

231.  Kemp, W. B., Jr.; R. E. Becht; and A. G. Few, Jr.
      "Stability and Control Characteristics at Low Speed
      of a 1/4-Scale Bell X-5 Airplane Model.  Longitudinal
      Stability and Control," NACA RM L9K08, 1950.

232.  Kemp, W. B., Jr. and A. G. Few, Jr.  "Pressure
      Distribution at Low Speed on a 1/4 Scale Bell X-5
      Airplane Model," NACA RM L51I25, Dec., 1951.

233.  Kemp, W. B., Jr.; R. E. Becht; and A. G. Few, Jr.
      "Investigation of the Low-Speed Aerodynamic Character-
      istics of a Variable-Sweep Airplane Model with a
      Twisted and Cambered Wing," NACA RM L51K22, Feb., 1952.

234.  Kemp, W. B., Jr.; R. E. Becht; and A. G. Few, Jr.
      "Stability and Control Characteristics at Low Speed
      of a 1/4-Scale Bell X-5 Airplane Model.  Longitudinal
      Stability and Control," NACA RM L9K08, March 14, 1950.

235.  Stillwell, W. H.  "X-15 Research Results with a Selected
      Bibliography," NASA SP-60, 1965.

I.  Boundary Layer Control on High-Speed Wings

236.  Anderson, S. B.; H. C. Quigley; and R. C. Innis.
      "Flight Measurements of the Low-Speed Characteristics
      of a 35° Swept-Wing Airplane with Blowing-Type Boundary-
      Layer Control on the Trailing-Edge Flaps," NACA RM
      A56G30, Oct., 1958.

237.  Bray, R. S. and R. C. Innis.  "Flight Tests of
      Leading-Edge Area Suction on a Fighter-Type Airplane
      with a 35° Sweptback Wing," NACA RM A55C07, June, 1955.

238.  Carriere, P.; E. Eichelbrenner; and P. Poisson-Quinton.
      "Theoretical and Experimental Contribution to the
      Study of Boundary Layer Control by Blowing," ADV.
      AERO. SCI., Vol. II, Pergamon Press, 1959.

239. Cook, W. L.; S. B. Anderson; and G. E. Cooper. "Area-Suction Boundary-Layer Control as Applied to the Trailing-Edge Flaps of a 35° Swept-Wing Airplane," NACA 1370, 1958.

240. Fink, M. P. and H. C. McLemore, "High-Pressure Blowing Over Flap and Wing Leading-Edge of a Thin Large Scale 49° Swept Wing-Body-Tail Configuration in Combination with a Drop Nose and Nose Radius Increment," NACA RM L57D23, May, 1957.

241. Gratzer, L. B. and T. J. Odonnel. "The Development of a BLC High Lift System for High Speed Airplanes," AIAA Paper 64-589, Transport Aircraft Des. and Op. Meeting, 1964.

242. Holzhauser, C. A. and R. K. Martin. "The Use of Leading-Edge Area-Suction Flap to Delay Separation to Air Flow from the Leading Edge of a 35° Sweptback Wing," NACA RM A53J26, Dec., 1953.

243. Hickey, D. H. and K. Aoyagi. "Large-Scale Wind Tunnel Tests of an Airplane Model with a 45° Sweptback Wing of AR= 2.8 Employing High Velocity Blowing Over the Leading-Edge and Trailing-Edge Flaps," NACA RM A58A09, May, 1958.

244. James, H. A. and R. L. Maki. "Low Speed Aerodynamic Characteristics of Swept-Wing Aircraft with Blowing Flaps and Leading-Edge Slats," NACA RM A57D11.

245. Kelly, M. W.; S. B. Anderson; and R. C. Innis. "Blowing-Type Boundary-Layer Control as Applied to the Trailing-Edge Flaps of a 35° Swept-Wing Airplane," NACA TR 1369, 1958.

246. Kelly, M. W.; W. H. Tolhurst, Jr.; and R. L. Maki. "Full-Scale Wind-Tunnel Tests of a Low-Aspect-Ratio, Straight-Wing Airplane with Blowing Boundary-Layer Control on Leading- and Trailing-Edge Flaps," NASA TN D-135, Sept. 1959.

247. Koenig, D. G. and K. Aoyagi. "The Use of a Leading-Edge Area-Suction Flap and Leading Edge Modification to Improve the High Lift Characteristics of an Air-plane Model with a Wing of 45° Sweep and AR= 2.8." NACA RM A57H21, Nov., 1957.

248. Maki, R. L. "Low-Speed Wind-Tunnel Investigation of Blowing Boundary-Layer Control on Leading- and Trailing-Edge Flaps of a Large-Scale, Low-Aspect-Ratio, 45° Swept-Wing Airplane Configuration," NASA Memo L-23-59A, Jan., 1959.

249. Maki, R. L. and D. J. Giulianetti. "Low-Speed Wind-Tunnel Investigations of Blowing Boundary Layer Control on Leading- and Trailing-Edge Flaps of a Full-Scale, Low-Aspect-Ratio, 42° Swept-Wing Airplane Configuration," NASA TN D-16, Aug., 1959.

250. McCormack, G. M. and W. L. Cook. "Effects of Boundary-Layer Control on the Longitudinal Characteristics of a 45° Swept-Forward Wing-Fuselage Combination," NASA RM A9K02a.

251. Pasamanick, J. and A. J. Proferra. "The Effect of Boundary-Layer Control by Suction and Several High-Lift Devices on the Longitudinal Aerodynamic Characteristics of a 47.5° Sweptback Wing-Fuselage Combination," NACA RM L8E18, 1948.

252. Pasamanick, J. and T. B. Sellers. "Full-Scale Investigation of Boundary-Layer Control by Suction Through Leading-Edge Slots on a Wing-Fuselage Con-figuration Having 47.5° Leading-Edge Sweep with and without Flaps," NACA RM L50B15, 1950.

253. Quigley, H. C.; S. B. Anderson; and R. C. Innis. "Flight Investigation of the Low-Speed Characteristics of a 45° Swept-Wing Fighter-Type Airplane with Blowing Boundary-Layer Control Applied to the Trailing-Edge Flaps," NACA RM A58E05, Aug., 1958.

254. Williams, J. and S. F. J. Butler. "Aerodynamic Aspects of Boundary Layer Control for High Lift at Low Speeds During Approach, Landing, and Takeoff - Aircraft Design and Handling," AGARD-414.

J. Miscellaneous

255. Brewer, J. D. "Description and Bibliography of NACA Research on Wing Controls, January, 1946 - February, 1955," NACA RM 54K24, March, 1955.

256. Sanders, K. L. "Subsonic Induced Drag," JOUR. AIRCRAFT, Vol. 2, No. 4, July-August, 1965.

257. Zimmerman, C. H. "Characteristics of Clark Y Airfoils of Small Aspect Ratio," NACA TR 431, 1932.

258. Snyder, M. H., Unpublished wind tunnel reflection-plane tests of delta wings and of B-52 wing conducted in the 7 x 10 Walter Beech Wind Tunnel at Wichita State University, 1965.

FIGURE 1
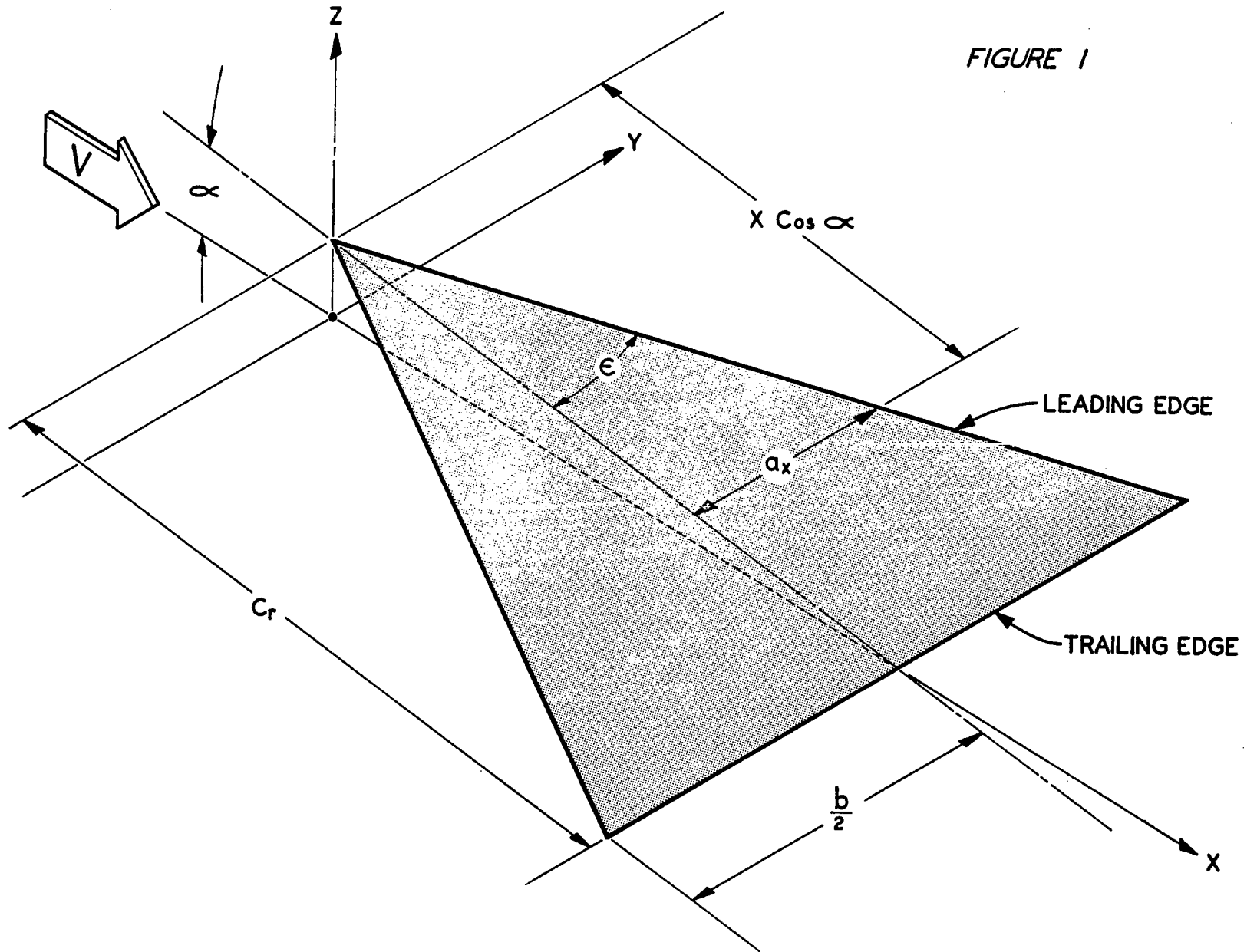
SLOPE OF THIS LINE, $\frac{d(C_l c)}{dy}$, IS PROPORTIONAL TO VORTICITY SHED AT THIS SPAN POSITION.

SPAN LOADING

$C_l c$

$\Gamma$

VORTEX FILAMENT SHEET
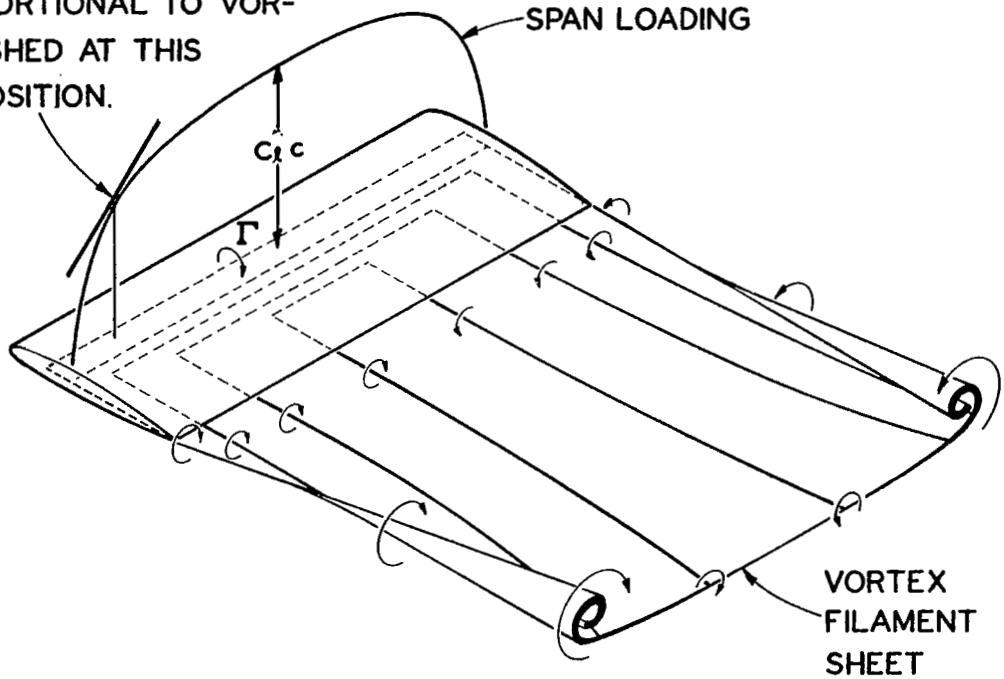
*FIGURE 2a*    RECTANGULAR PLAN FORM WING AT LIFT COEFFICIENTS WELL BELOW THE STALL.
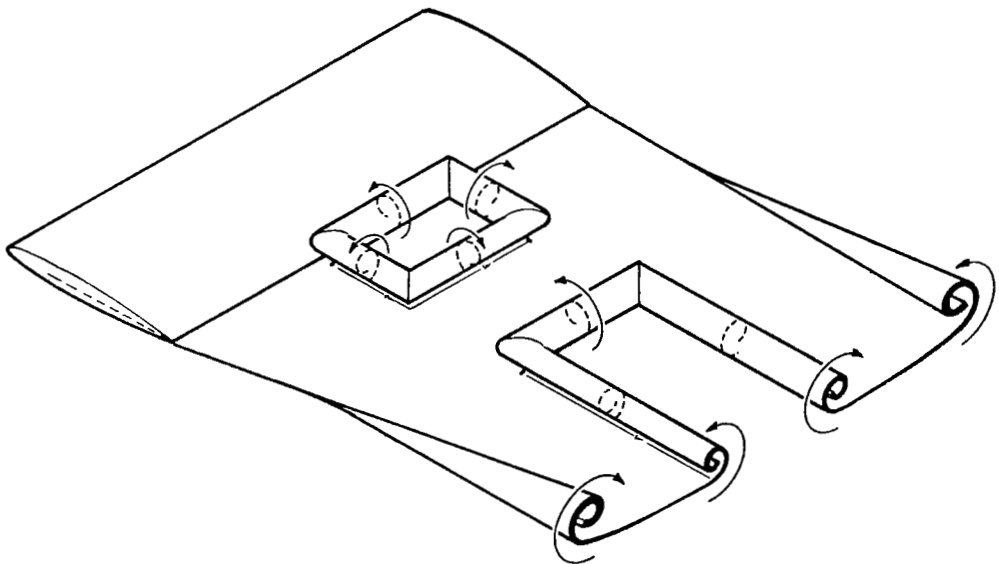


*FIGURE 2b*    RECTANGULAR PLAN FORM WING WITH INTERMITTENT TRAILING EDGE STALL AT THE CENTER SECTION.

TRAILING VORTEX SHEETS

BOUND VORTEX

CASE a

SEPARATED VORTEX SHEET

BOUND VORTEX

CASE b

BOUND VORTEX

SEPARATED VORTEX SHEET

CASE c

FIGURE 3

STALLED REGION

$\Gamma = f(C_\ell\, c)$

VIEW FROM BEHIND TRAILING EDGE
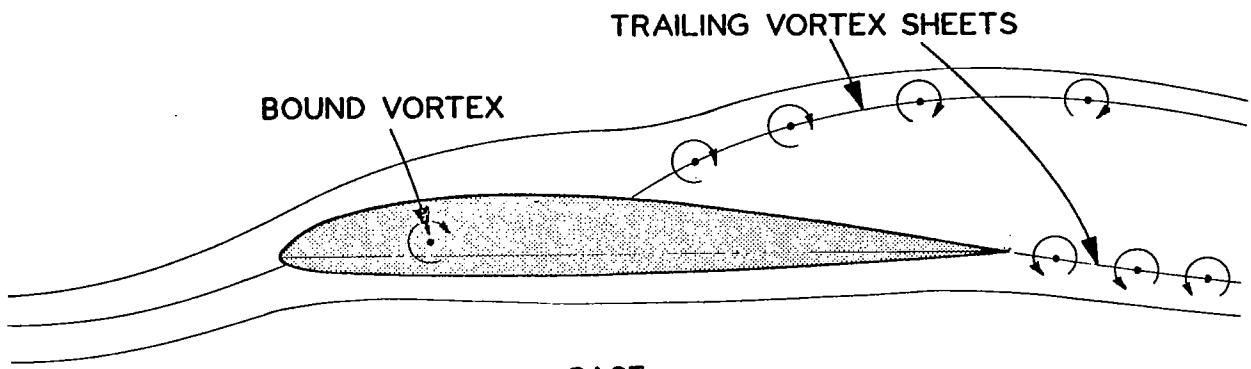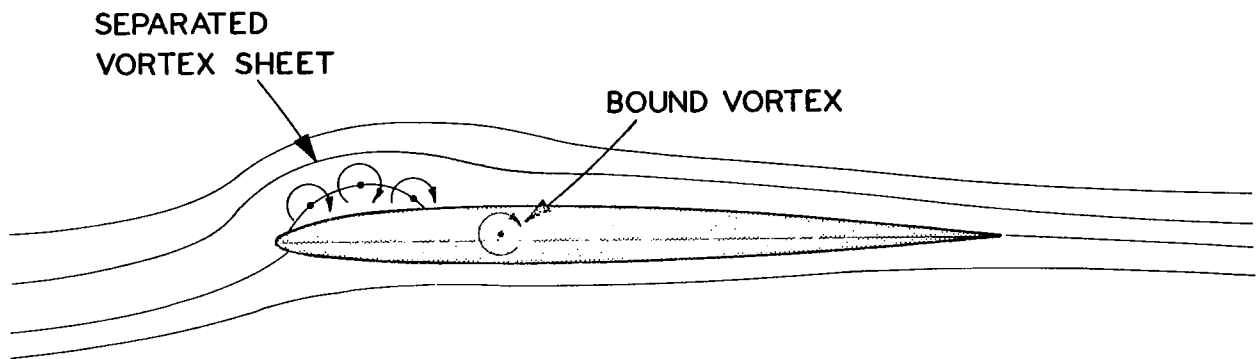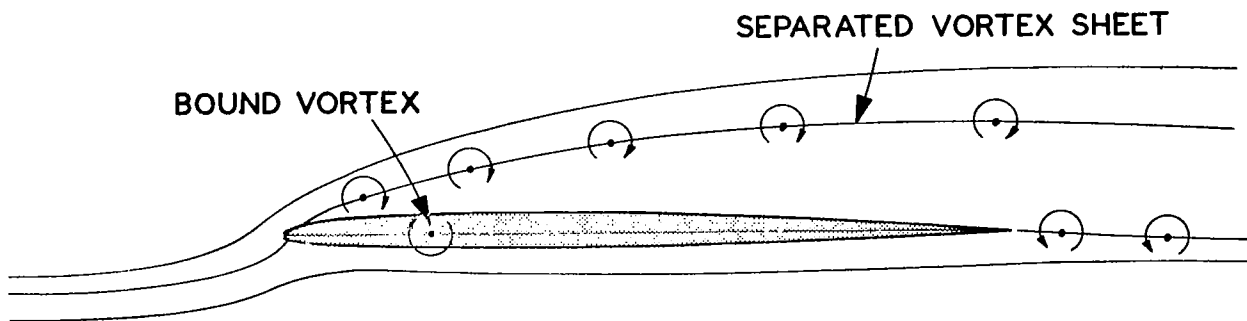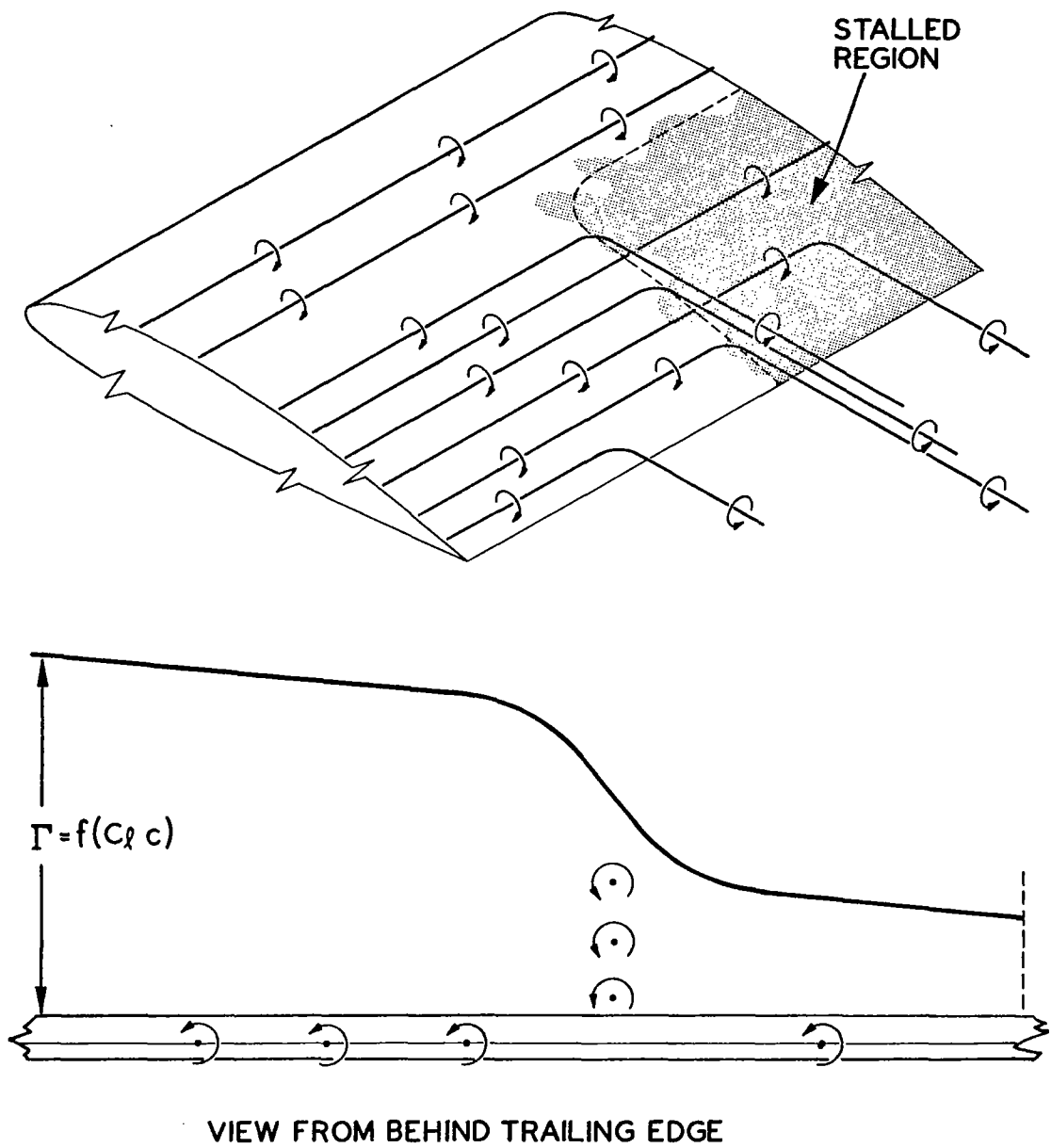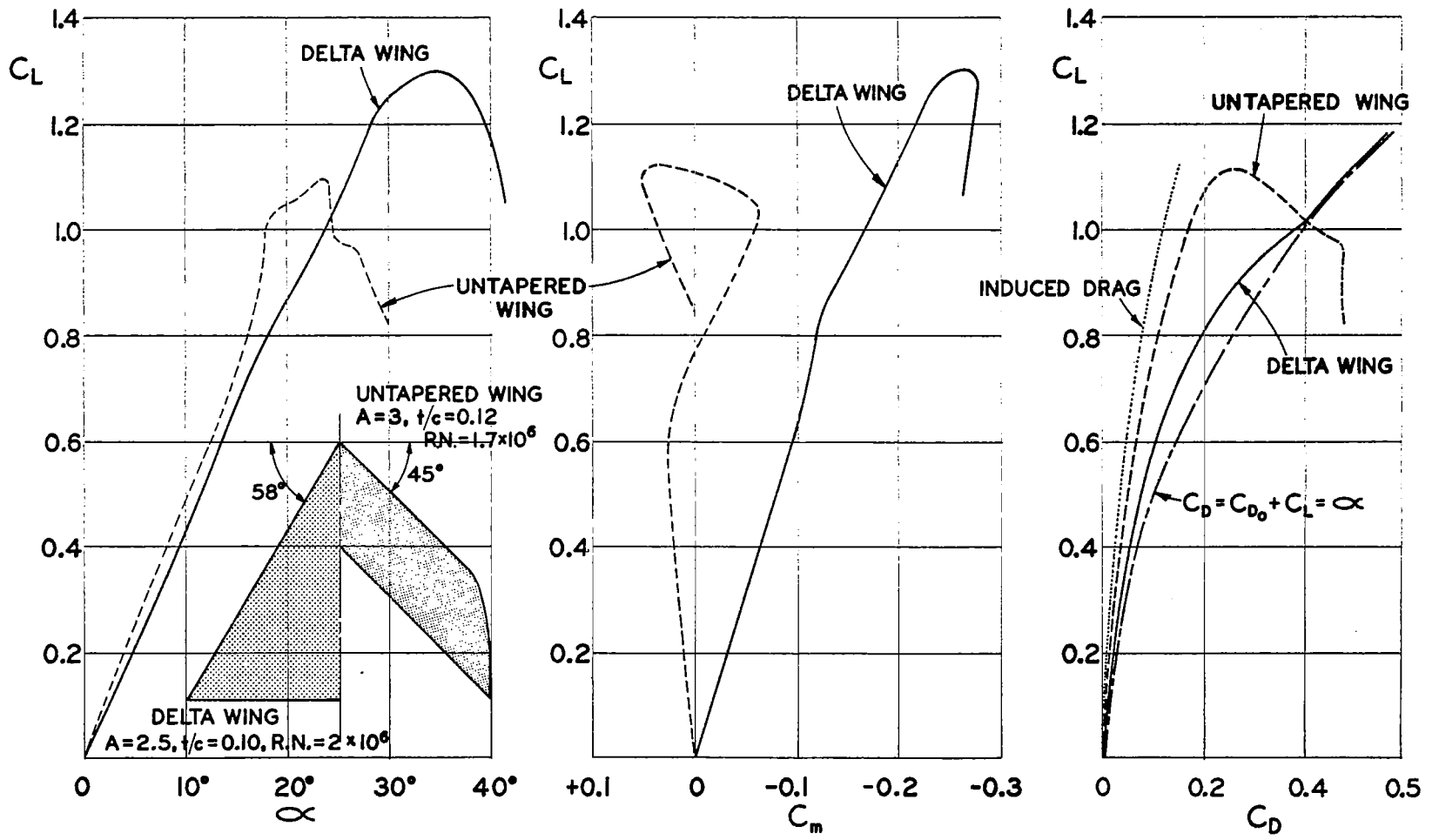
FIGURE 4

FIGURE 5    OVERALL FORCES AND MOMENTS ON A DELTA WING AND ON
AN UNTAPERED WING.

(FROM FIGURE 16 OF REFERENCE 71)
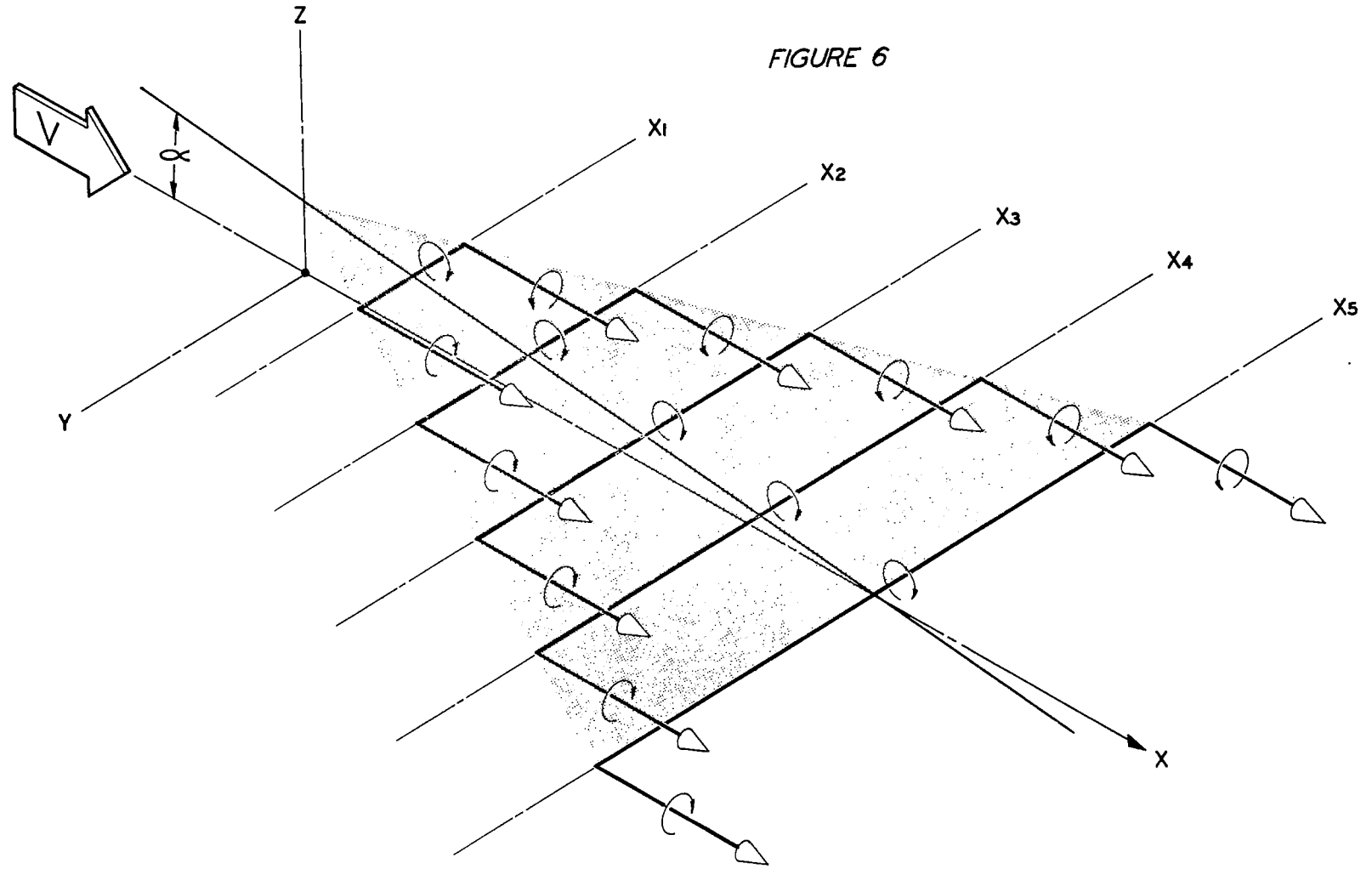
FIGURE 6
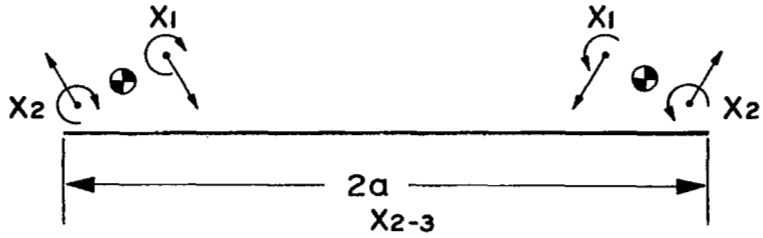
SECTION BETWEEN $X_2$ AND $X_3$

(a)
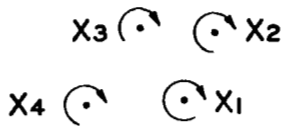
SECTION BETWEEN $X_4$ AND $X_5$

(b)                                                    (c)

TRANSVERSE SECTIONS THROUGH FIGURE 6

FIGURE 7

# SCHEMATIC DRAWINGS OF SEPARATED FLOW OVER SLENDER DELTA WINGS
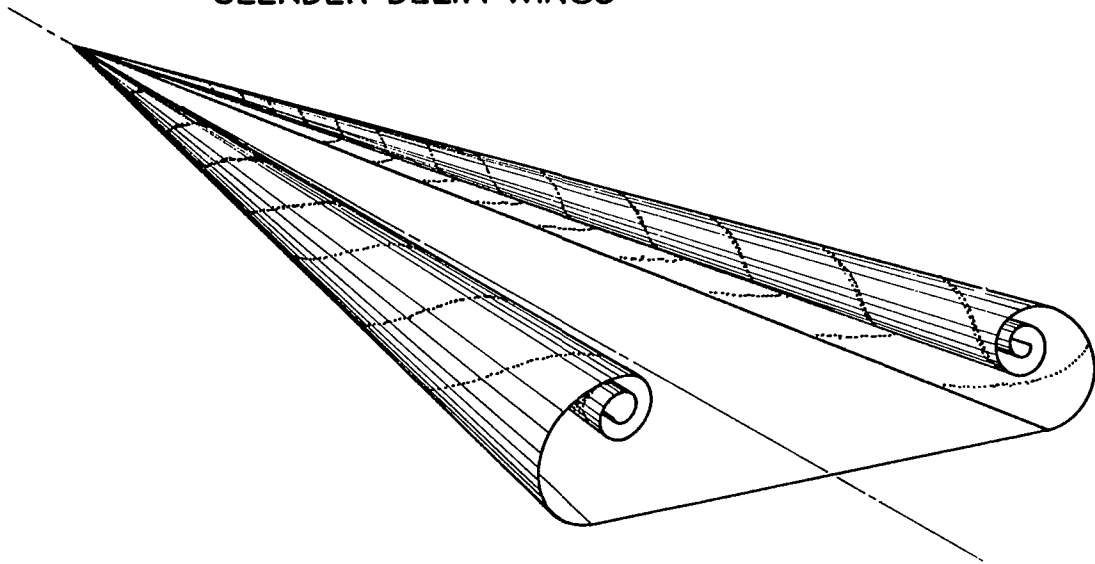


(a) ASSUMED FLOW FIELD
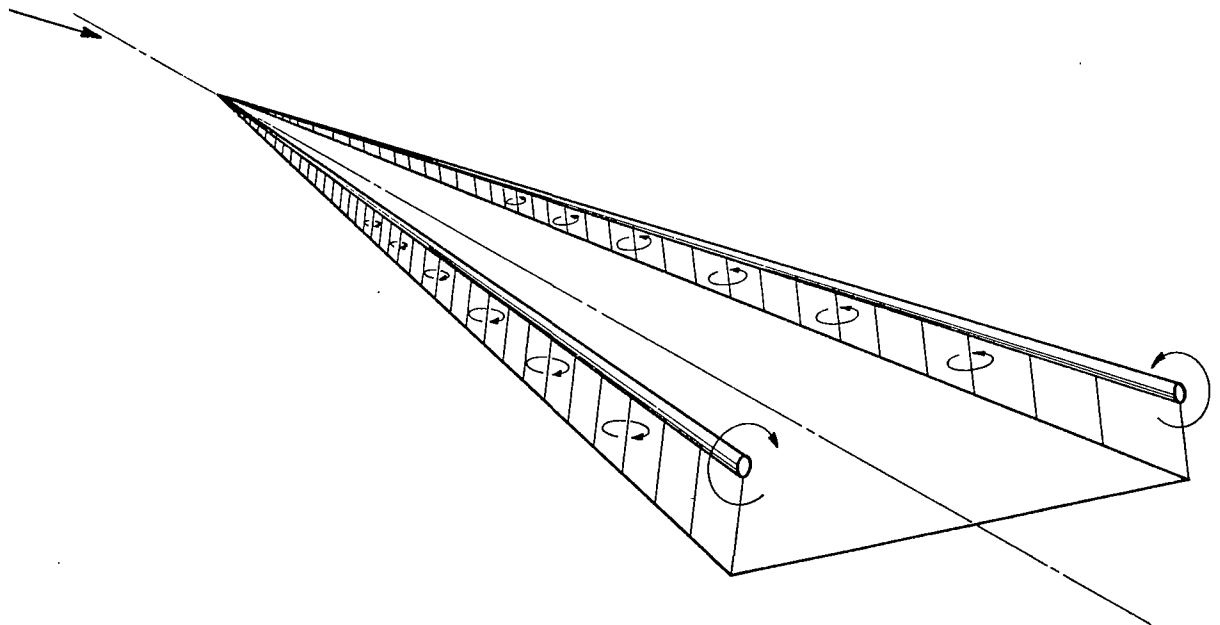


(b) APPROXIMATED FLOW FIELD

FIGURE 8

FROM REF.: NACA TECHNICAL NOTE 3430, PAGE 18, FIGURE 1

FIGURE 9



SPIRAL VORTEX SHEET SHED
FROM LEADING EDGE

INITIAL FORMATION OF
SECONDARY VORTEX

FULLY DEVELOPED
SPIRAL VORTEX

FULLY DEVELOPED
SECONDARY VORTEX
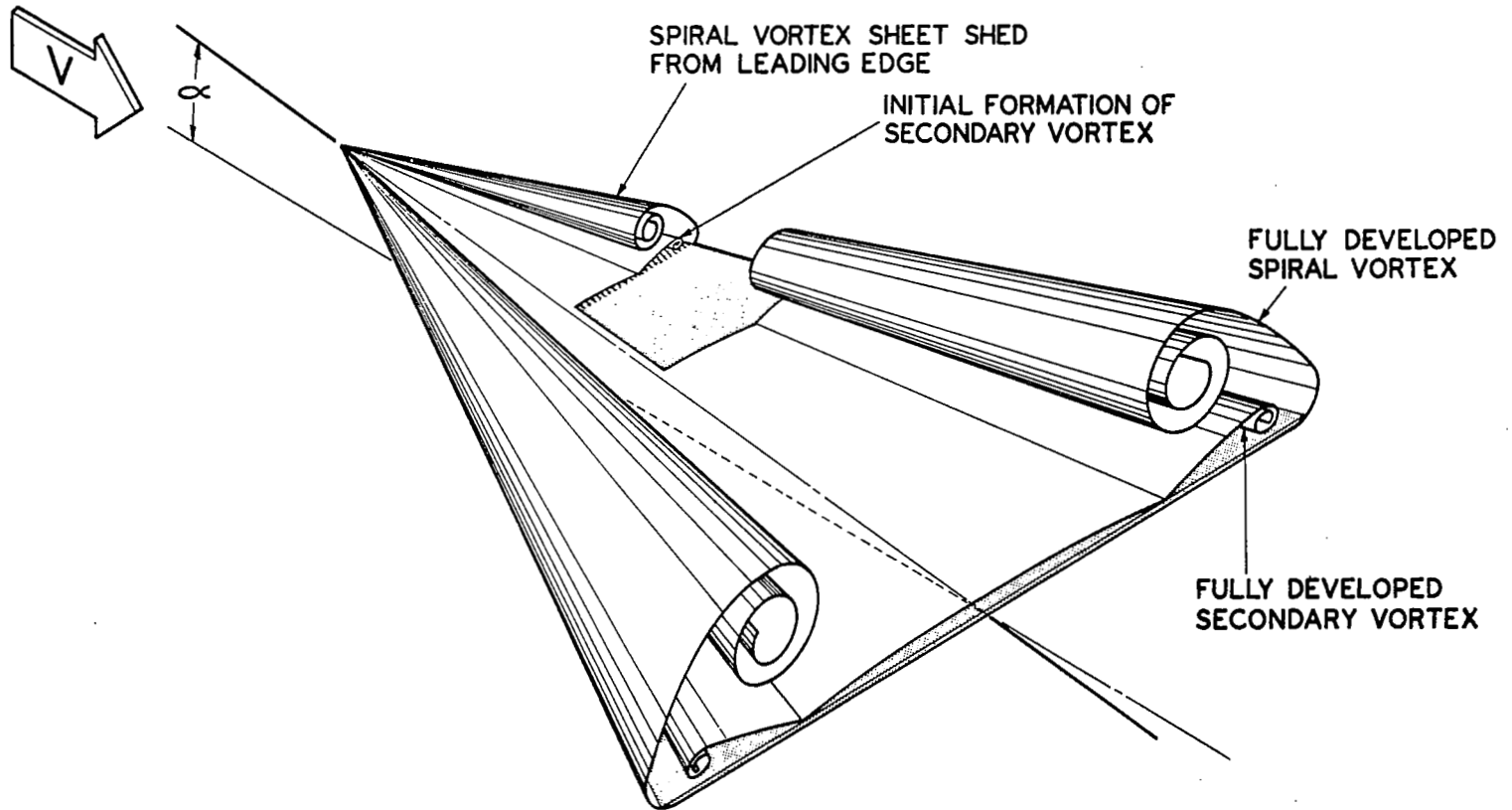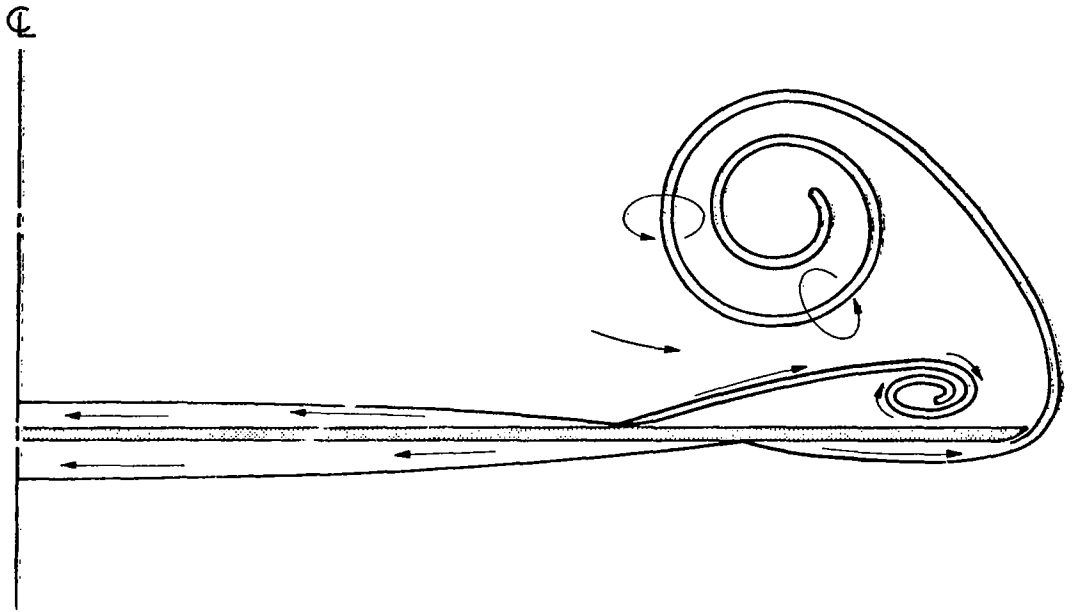
FIGURE 10

FLAT PLATE DELTA: VOTICES FROM TRAILING EDGE TO 0.50 Cr DOWN-
STREAM OF TRAILING EDGE.



(a) TRAILING EDGE

(b) 0.10 Cr DOWNSTREAM

(c) 0.20 Cr DOWNSTREAM

(d) 0.30 Cr DOWNSTREAM

(e) 0.40 Cr DOWNSTREAM

(f) 0.50 Cr DOWNSTREAM

*FIGURE II*

FROM REF: PRINCETON REPORT No. 510, FIGURE II, PAGES 35, 36,
AND 37.

FIGURE 12a

ANGLE OF ATTACK∝,DEGREES
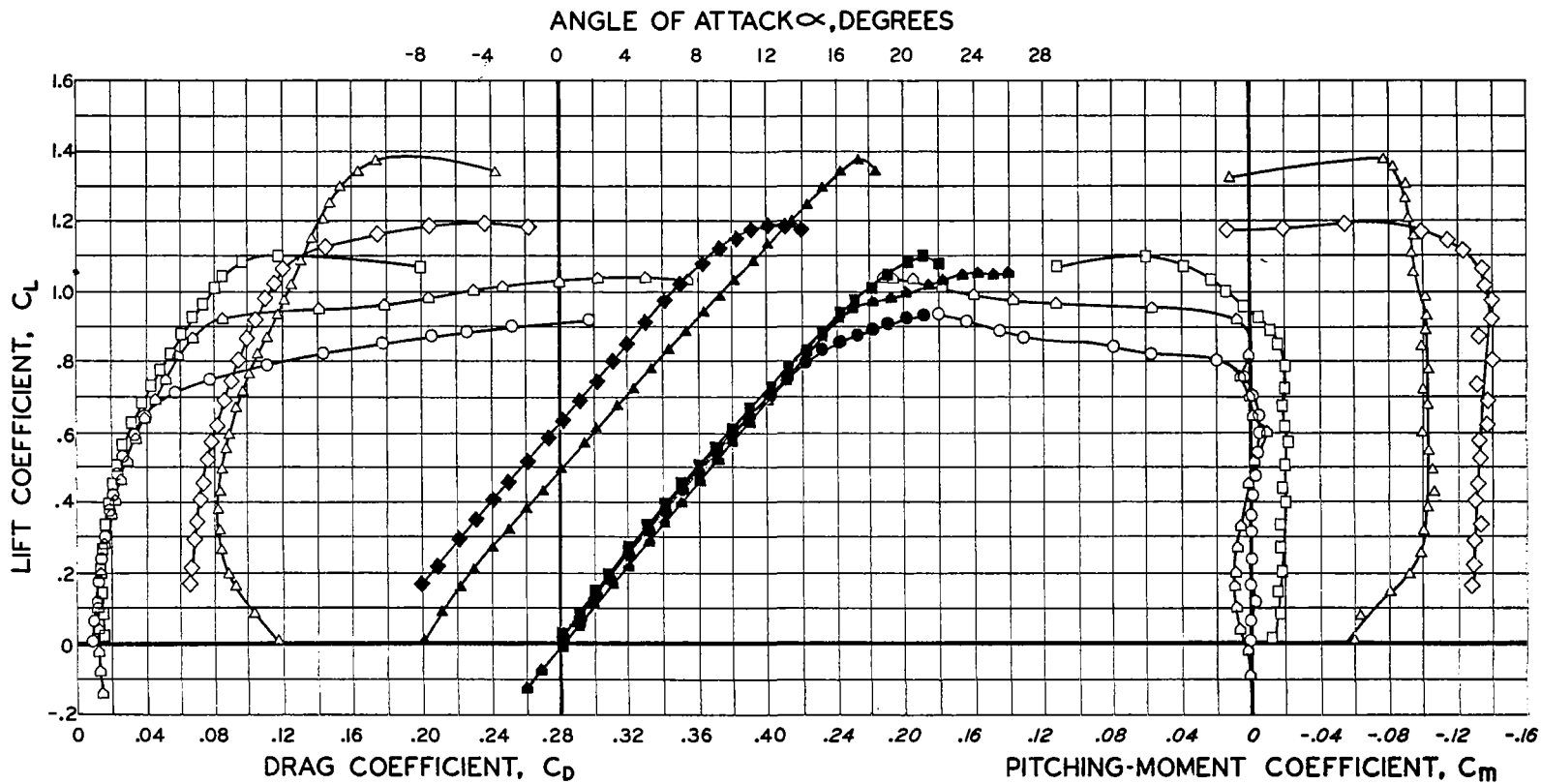


● OR ○ = PLAIN WING
■ OR □ = CAMBERED, TWISTED WING
● OR ◇ = PLAIN WING WITH FLAPS
▲ OR △ = CAMBERED, TWISTED WING WITH FLAP
● OR △ = PLAIN WING WITH L. E. DROOP

AERODYNAMIC CHARACTERISTICS OF PLAIN SWEPT
BACK WINGS, CAMBERED AND TWISTED WINGS, WITH AND
WITHOUT DOUBLE SLOTTED FLAPS.

(FROM FIGURES 4 AND 5 OF REFERENCE 173)

FIGURE 12b

$C_L$

α
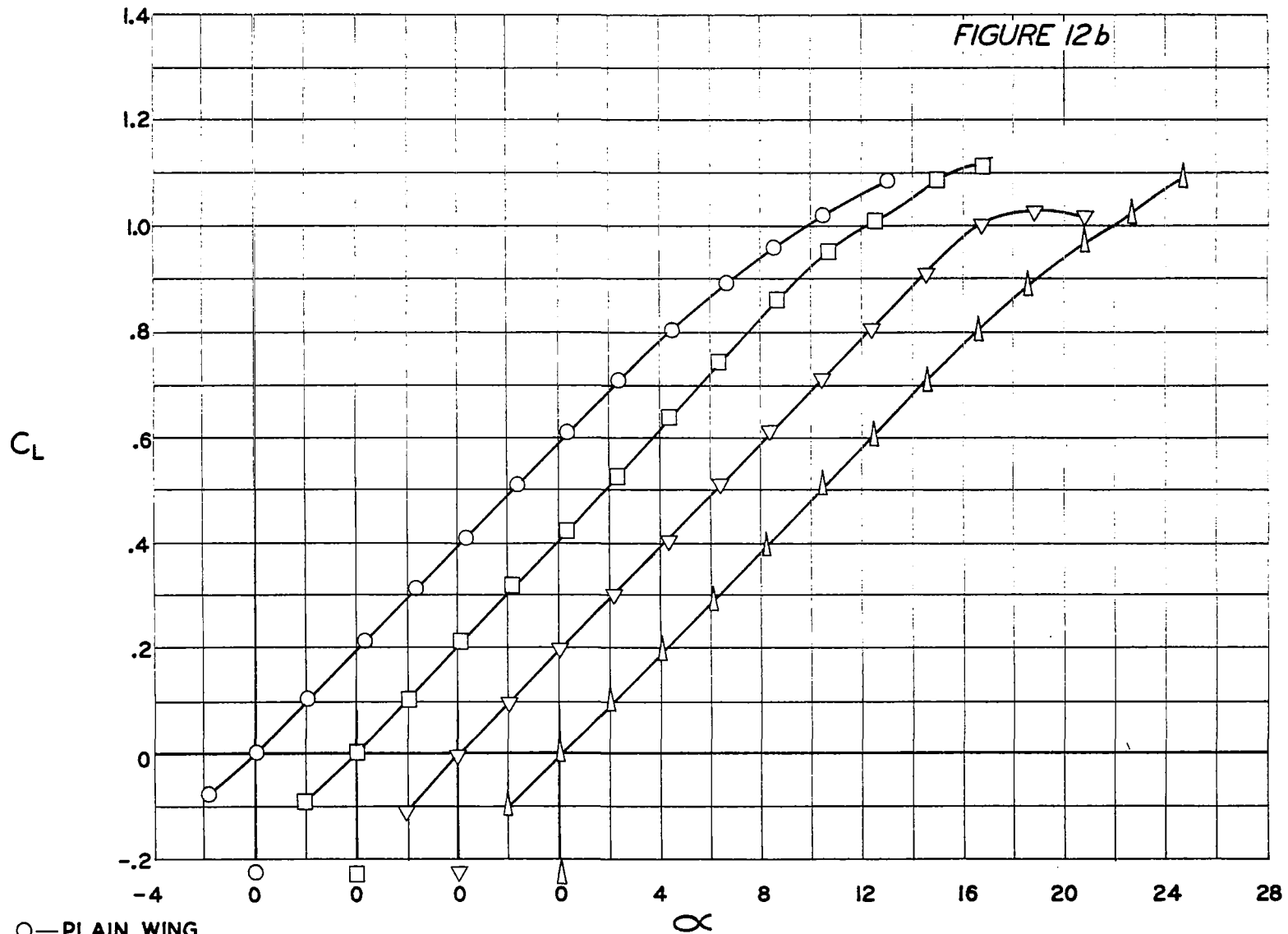
O—PLAIN WING
□-LEADING EDGE DROOP
▽—LEADING EDGE FLAP
△-LEADING EDGE EXTENSION

LIFT CHARACTERISTICS OF A DELTA WING
(FROM FIGURE 7b OF REFERENCE 113)

$C_{L_{max}}$

1.2

1.0

.8

.6

$C_{L_{max}}$ OF DELTA WINGS

--▲-- TOSTI, REF. 151

--▽-- GRAHAM, REF. 102

.4

.2

.0

0          1          2          3          4
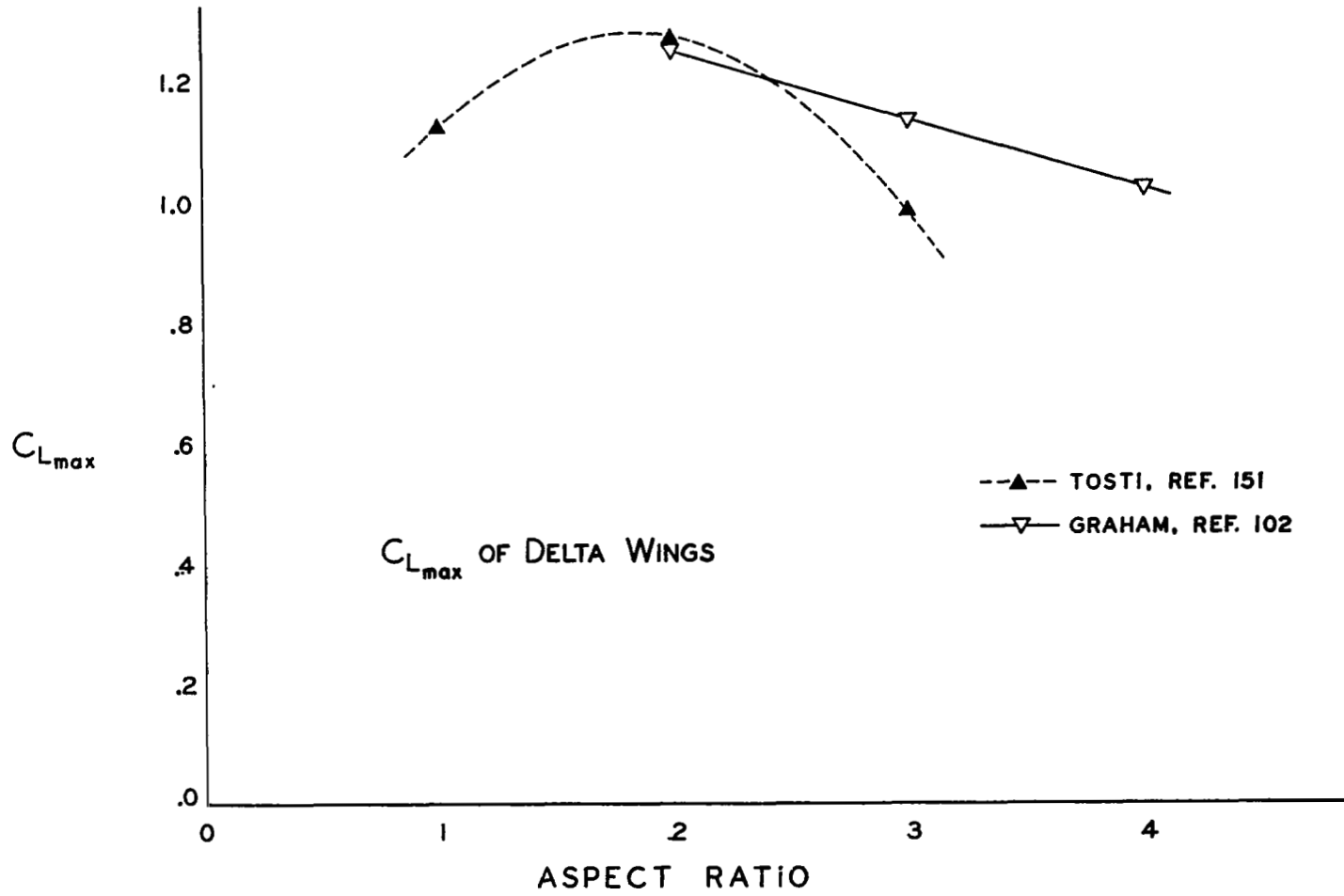
ASPECT RATIO
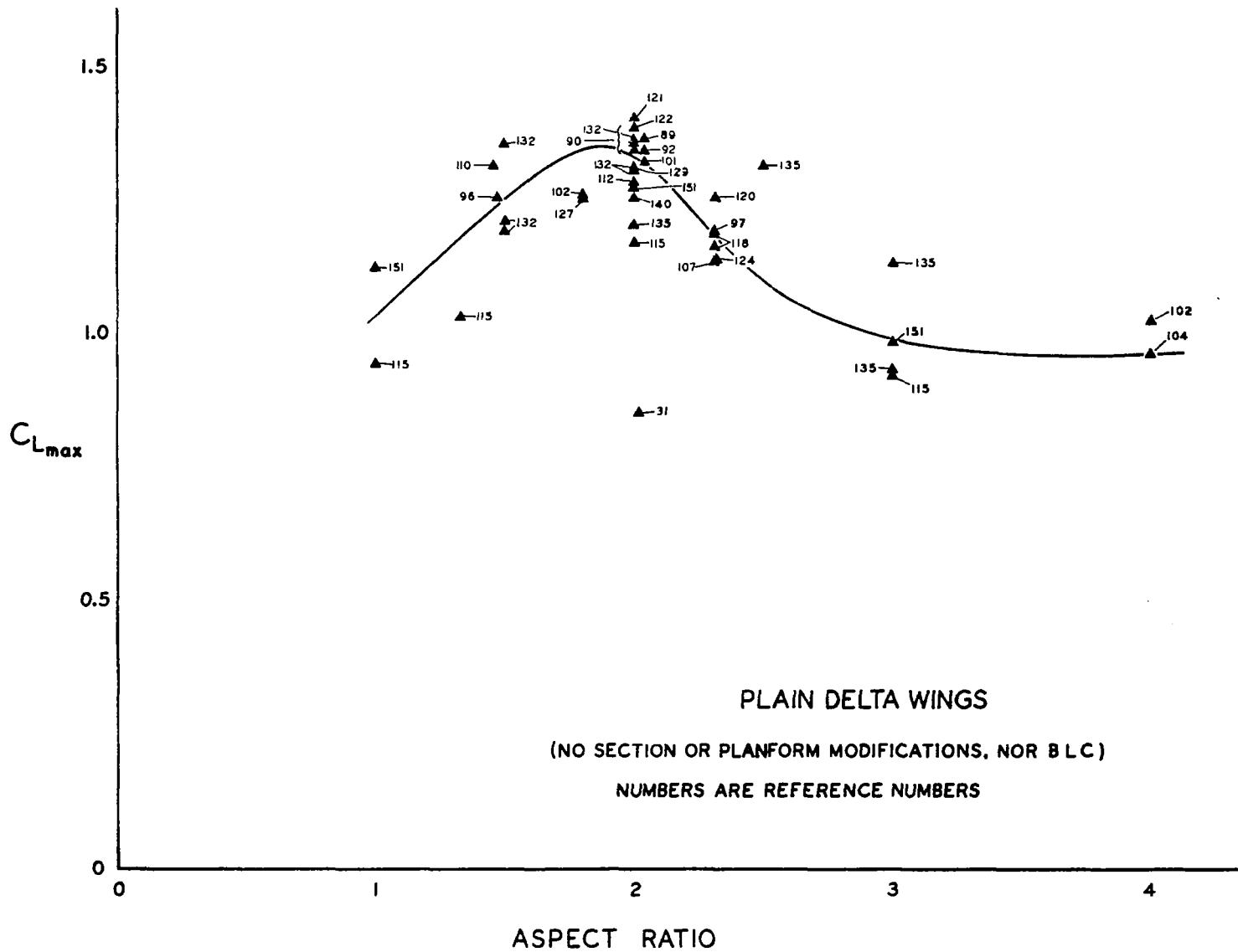
FIGURE 13

PLAIN DELTA WINGS

(NO SECTION OR PLANFORM MODIFICATIONS, NOR B L C)

NUMBERS ARE REFERENCE NUMBERS

FIGURE 14

77

FIGURE 15

FIGURE 16

$C_{L_{max}}$ OF DELTA WINGS

$\Lambda$, SWEEPBACK ANGLE OF LEADING EDGE, DEGREES
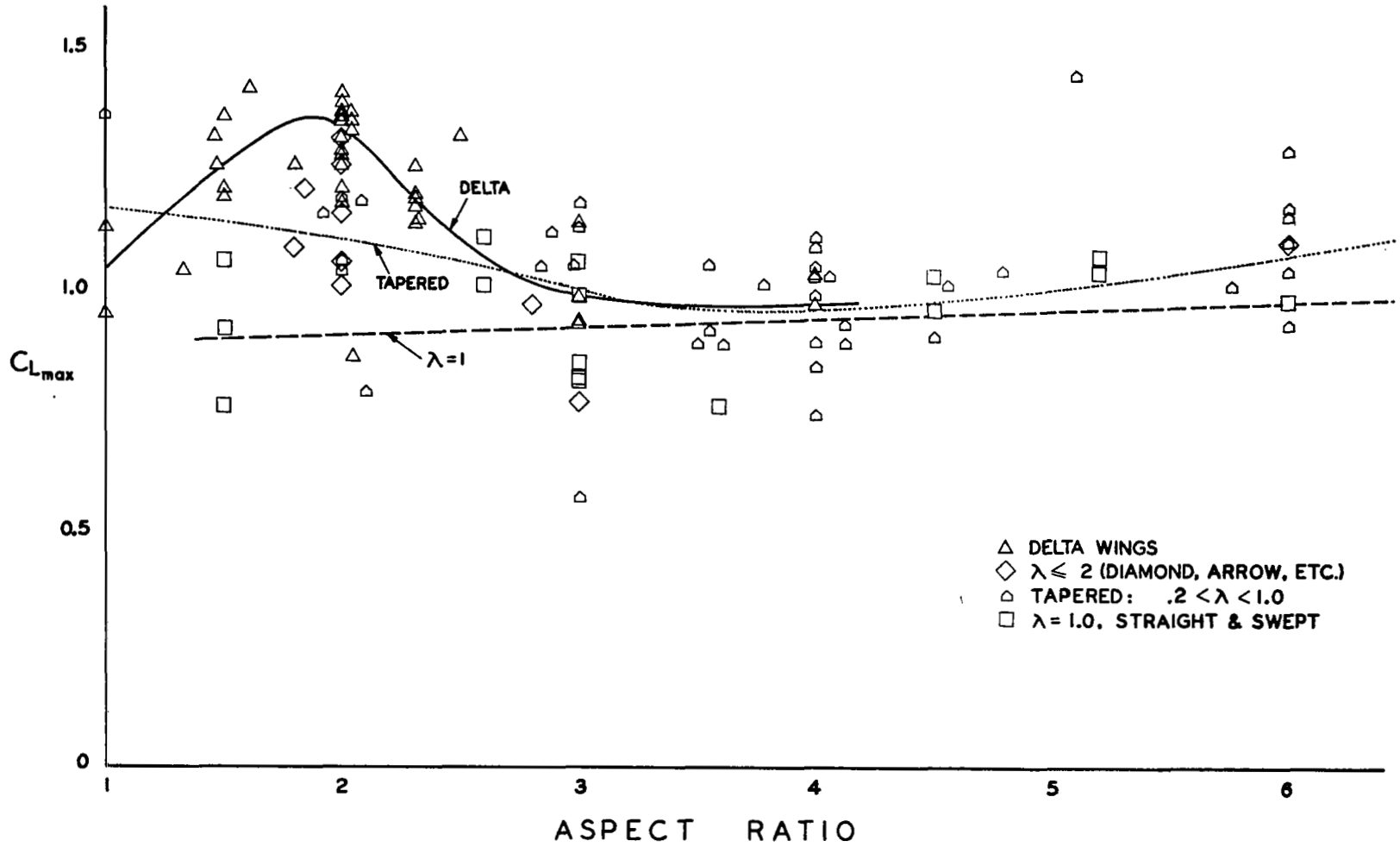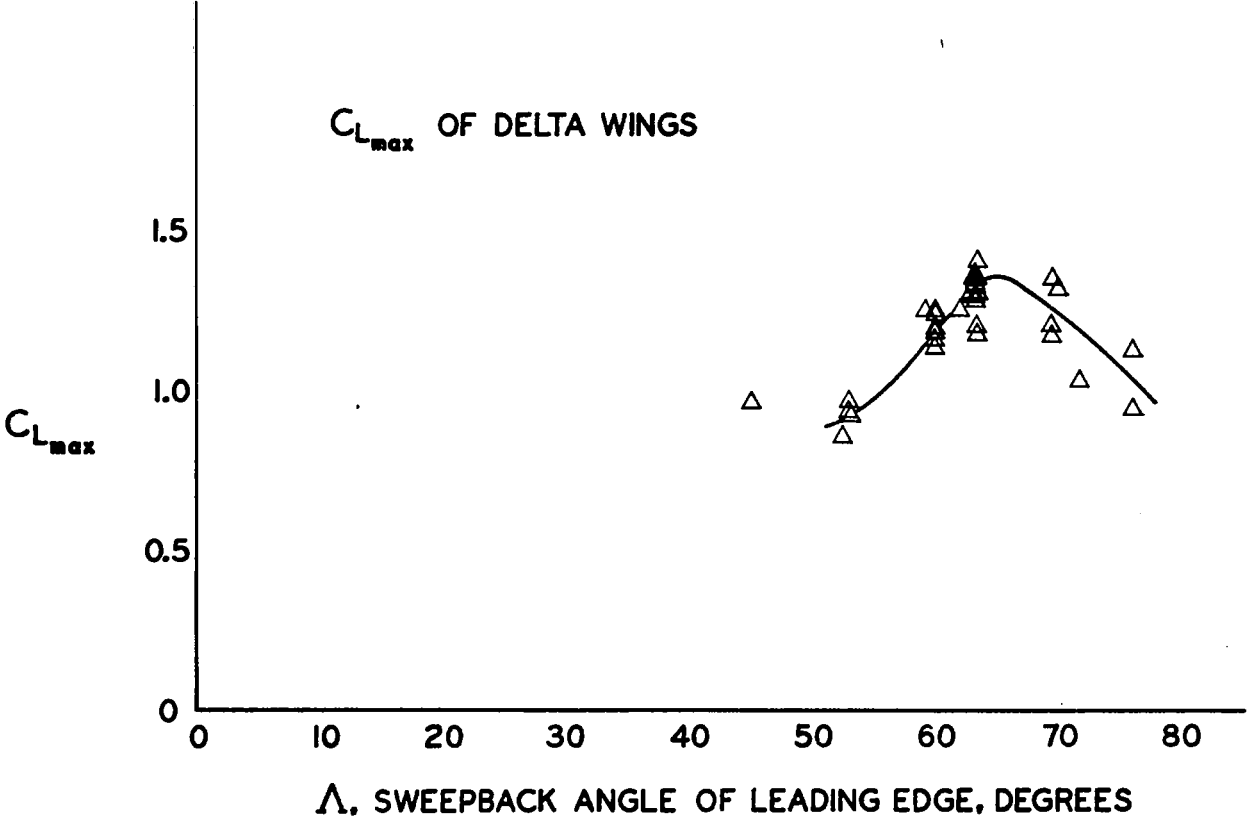
FIGURE 17

VARIATION OF $C_{L_{max}}$ WITH SWEEPBACK
FOR WINGS HAVING PLANFORMS OTHER
THAN TRIANGULAR.

SYMBOL  ASPECT RATIO RANGE
○——— 1.8 – 2.2
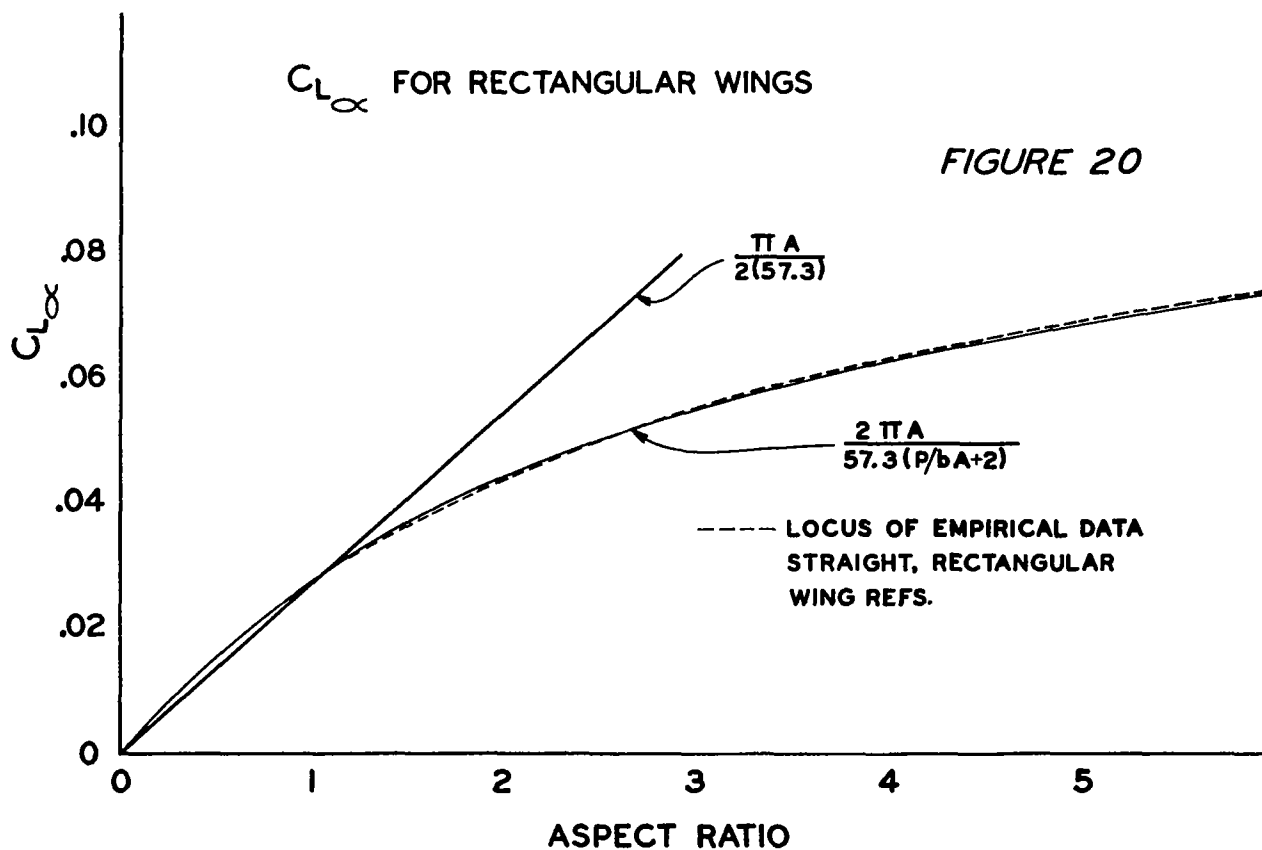⌂——— 2.7 – 3.3
□——— 3.6 – 4.4
◇——— 5.4 – 6.6

——————— APPARENT TREND – NON-DELTA PLANFORM
- - - - - - - TREND OF DELTA WINGS

Λ, LEADING EDGE SWEEPBACK ANGLE
(IN DEGREES)

FIGURE 18

FIGURE 19

$\frac{C_{L_{max}}}{A}$

Θ, OUTBOARD SWEEP ANGLE, DEGREES

O LARGE ASPECT RATIO MODEL
□ SMALL ASPECT RATIO MODEL
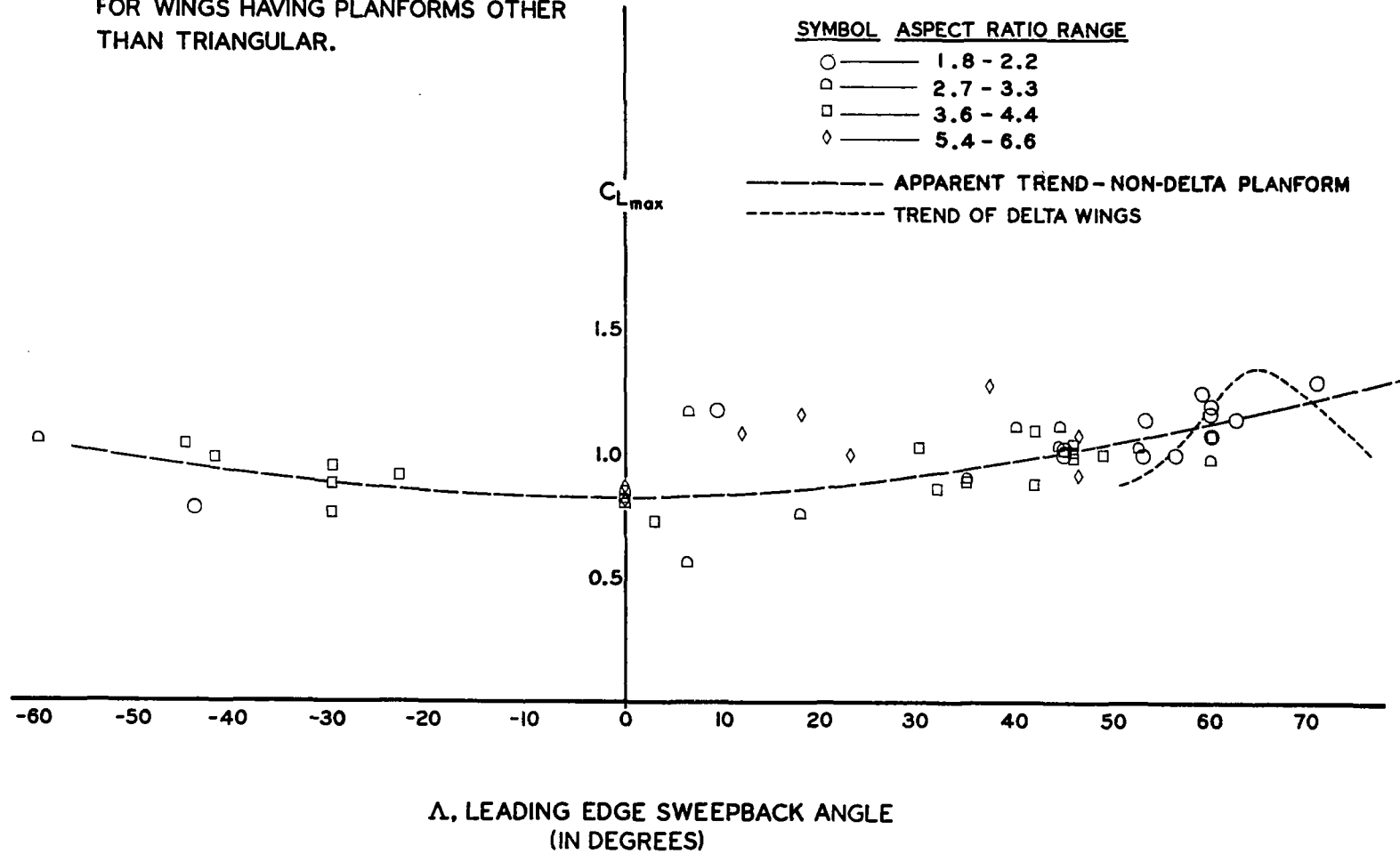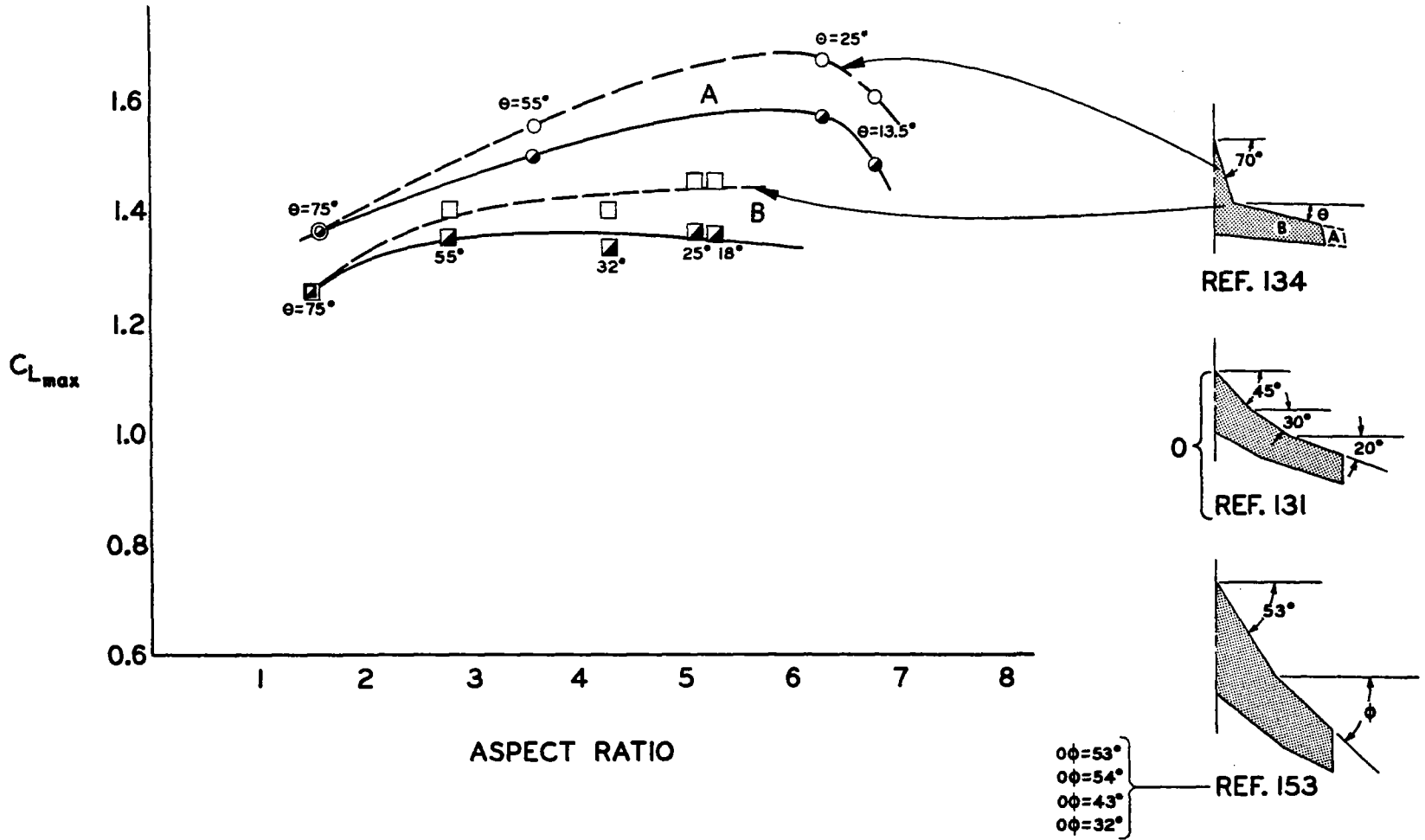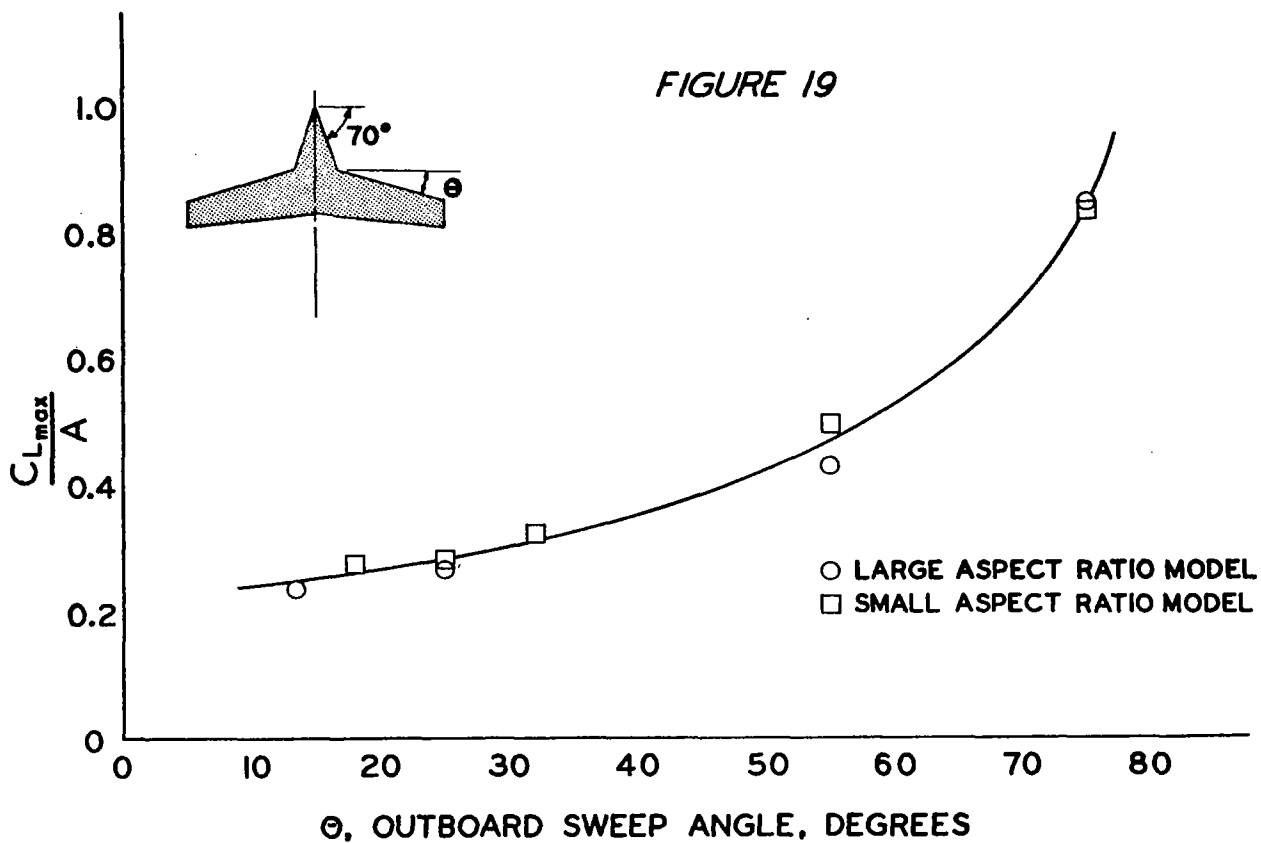


$C_{L_\alpha}$ FOR RECTANGULAR WINGS

FIGURE 20

$C_{L_\alpha}$

$\frac{\pi A}{2(57.3)}$

$\frac{2\pi A}{57.3(P/bA+2)}$

---- LOCUS OF EMPIRICAL DATA
STRAIGHT, RECTANGULAR
WING REFS.

ASPECT RATIO

82

DELTA WINGS

Figure 21

LOW ASPECT RATIO PREDICTION – SEE R.T.JONES, NACA REPORT 835
WEISSINGER METHOD – FROM DE YOUNG & HARPER, NACA REPORT 921
EQUATION (A)

$C_{L_\alpha}$ (at $C_L$ = 0)

.07
.06
.05
.04
.03
.02
.01

△ DELTA WINGS – PUBLISHED DATA FROM NACA RM'S
O PARAWINGS WITH TRIANGULAR PLANFORM
□ FROM FIGURE A,7U, JONES & COHEN, "HIGH SPEED WING THEORY"

ASPECT RATIO

0    1    2    3    4    5

FIGURE 22

$$C_{L_\alpha} = \frac{\pi A}{2(57.3)}$$

VARIATION OF LIFT-CURVE SLOPE WITH ASPECT
RATIO FOR VARIOUS VALUES OF SWEEP AND TAPER
RATIO.

FIGURE 23

TAPERED WINGS

FIGURE 24

FIGURE 25

$\frac{dC_L}{d\alpha}$ AT $C_L$=0.8 FOR DELTA WINGS

$\frac{dC_L}{d\alpha}$ AT $C_L$=0.8

(PER DEGREE)

APPARENT  TREND OF DATA

$C_{L\alpha}$ FOR DELTA WINGS, FIGURE 21

$\frac{\pi A}{2(57.3)}$

ASPECT  RATIO

FIGURE 26

$\frac{dC_L}{d\alpha}$ AT $C_L$=.8 FOR TAPERED WINGS

FIGURE 27



DELTA WING, $\Lambda = 62°$, $A = 1.8$
(SEE REFERENCE 258)

$\triangle$ AT POSITIVE $\alpha$
$\triangledown$ AT NEGATIVE $\alpha$
----- $.01 + C_L \tan \alpha$
--.--. $.01 + \dfrac{C_L^2}{\pi A}$

$C_D$

$C_L^2$

FIGURE 28

NOSE FLAPS (DROOP) ON A DELTA WING (WITH FUSELAGE), A $= 2$
(DATA FROM REFERENCE 129)

FIGURE 29

$C_{D_o} + C_L$ TAN $\propto$

$C_{D_o} + C_L^2 / \pi A$

$S_f = 0$

$S_f = 40°$

$S_f = 60°$

$C_D$

$C_L$

FIGURE 30

$D/L$ AT $C_L = 0.8$ FOR DELTA WINGS

F 5D COMPLETE AIRPLANE

$D/L$ AT $C_L = 0.8$

$\Lambda$, DEGREES

FIGURE 31

D/L AT $C_L = 0.8$ FOR SWEPT-BACK WINGS

$\Lambda = 60°$

DELTAS FROM FIGURE 30

$\Lambda = 45°$

$\Lambda = 0°$

ASPECT RATIO

D/L

*FIGURE 32*

D/L AT $C_L$ = 0.8 FOR VARIABLE-SWEEP WINGS

(REFERENCE 134)

O HIGH ASPECT RATIO MODEL A
□ LOW ASPECT RATIO MODEL B

ASPECT RATIO

FIGURE 33

REFLECTION PLANE DELTA WING
TESTS WITH FUSELAGE
DATA FROM W.H. WENTZ
WICHITA STATE UNIVERSITY 1965
(REFERENCE 126)

62°-80° DOUBLE DELTA

62°-75° DOUBLE DELTA

62° DELTA

$C_L = .8$

$C_D$

$C_L^2$